

SFB/CPP-14-101
DESY 15-006

Non-perturbative Heavy Quark Effective Theory: Introduction and Status

Rainer Sommer^{a,b}

^a*John von Neumann Institute for Computing (NIC), DESY, Platanenallee 6, 15738 Zeuthen, Germany*

^b*Institut für Physik, Humboldt Universität, Newtonstr. 15, 12489 Berlin, Germany*

Abstract

We give an introduction to Heavy Quark Effective Theory (HQET). Our emphasis is on its formulation non-perturbative in the strong coupling, including the non-perturbative determination of the parameters in the HQET Lagrangian. In a second part we review the present status of HQET on the lattice, largely based on work of the ALPHA collaboration in the last few years. We finally discuss opportunities and challenges.

Keywords: Lattice QCD, Heavy Quark Effective Theory, Bottom quarks, Meson decay

PACS: 11.15.Ha, 12.38.Gc, 12.39.Hg, 14.65.Fy, 13.20.He, 13.20.-v, 12.15.Ff

Contents

1	Introduction	1
1.1	Mass scaling and phenomenology . . .	2
1.2	Heavy quarks in lattice QCD	2
1.3	Defining effective field theories beyond perturbation theory	3
1.4	HQET	4
1.5	Heavy quark symmetries	4
1.6	Theoretical status	5
1.7	HQET parameters	6
2	Matching and mass scaling	6
2.1	One-loop perturbation theory	6
2.2	Higher orders in the coupling and renor- malization group invariants	9
2.3	On the accuracy of perturbation theory .	11
2.4	Matching at NLO in $1/m_h$	11
2.5	Non-perturbative matching	12
3	Discretized HQET	14
4	Verification of HQET	15

5	Numerical Simulations and results	17
5.1	The $B^*B \pi$ coupling.	18
5.2	HQET parameters	18
5.3	Mass of the b-quark	20
5.4	B-meson decay constants	21
6	Conclusions, opportunities and challenges	26

1. Introduction

Heavy Quark Effective Theory (HQET) is an effective theory for QCD, the theory of strong interactions, in the limit where quark masses are large and other scales, such as momenta are kept fixed. Understanding this limit is of great interest per se. In addition a control of HQET is very useful to arrive at phenomenological predictions for B-meson properties and qualitatively also for D-mesons. In particular B-meson decays need to be understood better in order to further constrain the flavor sector of the standard model of particle physics.

In this article we give an introduction to HQET with an emphasis on its full non-perturbative formulation. Mostly we remain with the general ideas and an overview of the present status and results. For more details concerning the basics as well as the phenomenology we refer to the literature [1, 2, 3, 4, 5] with the non-perturbative aspects and particularly the discretisation on a lattice covered in the last reference. Here, on the other hand, we give a more complete discussion of the status and of non-perturbative computations and the challenges for the future.

HQET, as discussed here, is an effective field theory for the low energy physics of energy levels or transition matrix elements with a single heavy quark or anti-quark in initial and/or final state. We will label these hadronic states by H and the quark by h . The latter has a mass m_h .¹ Usually we think of H as a B-meson, but it can be e.g. a baryon with beauty quantum number of one. We always consider a rest-frame where all spatial momenta \mathbf{p}_i are small. The effective theory then yields the expansion of observables of QCD in powers

$$(|\mathbf{p}_i|/m_h)^n, (\Lambda/m_h)^n, (m_j/m_h)^n \quad (1)$$

where h is a heavy quark, while the masses m_j of the other quarks are considered small.²

1.1. Mass scaling and phenomenology

The HQET expansion is of a **theoretical interest** because it describes the asymptotics of QCD as $m_h \rightarrow \infty$. For example we obtain statements such as

$$\mathcal{M}_{\text{QCD}}(\{\mathbf{p}_i\}, \{m_j\}, m_h) = \mathcal{M}^{\text{stat}}(\{\mathbf{p}_i\}, \{m_j\}, m_h) \times (1 + \mathcal{O}(1/m_h)) \quad (2)$$

with $\mathcal{O}(1/m_h)$ summarizing the terms of eq. (1). The intrinsic scale Λ may be taken to be any low energy QCD scale.

The important content of eq. (2) is that it gives the large mass scaling of observables \mathcal{M}_{QCD} with m_h , in the form of the static (lowest order) of HQET prediction, usually

$$\mathcal{M}^{\text{stat}} \sim (m_h)^s \quad (3)$$

with the (not necessarily integer) power s determined by counting dimensions and adding anomalous ones in

the static effective theory. Understanding this scaling is clearly a very relevant part of understanding QCD.

A second important motivation for studying (and computing in) HQET is that the b-quark mass, say in the $\overline{\text{MS}}$ scheme at 4 GeV renormalization scale, is of order 4 GeV. It is an order of magnitude larger than the intrinsic QCD scale of around $\Lambda \approx 400$ MeV. Indeed, if one wants the $\mathcal{O}(1/m_h)$ to give a first estimate of the numerical size of the corrections (without additional pre-factors) this value for Λ is appropriate in eq. (1) as we will see in section 5. Consequently, as long as we keep momenta small, static predictions are expected to be good at the 10% level and one has an accuracy at the 1% level when $1/m_h$ corrections are included. Thus HQET is a very interesting **phenomenological tool**.

1.2. Heavy quarks in lattice QCD

One may still wonder why it is of interest in the context of lattice QCD. The reason is simply that a numerical lattice QCD computation necessarily is done with an infrared cutoff $1/L$ through the linear extent L of the simulated $T \times L^3$ world on top of the ultraviolet cutoff $1/a$ introduced by the lattice spacing a . The accessible physical energies E_i have to be removed from these scales,

$$1/L \ll E_i \ll 1/a, \quad (4)$$

otherwise properties of the associated states are distorted.

In table 1 we list the most relevant effects that are at the origin of these bounds as well as the errors which result from violating them. Since the finite volume effects are exponential in L , the bound of $m_\pi L = 4$ is rather sharp. However it depends on the pion mass m_π which one has in the simulation. Reasonable values of $m_\pi = 300 \text{ MeV} \dots 150 \text{ MeV}$ lead to $L \geq 2.5 \text{ fm} \dots 5 \text{ fm}$.

In contrast discretisation errors only disappear like a^2 . Further they vary a lot depending on the quantity and discretised action. They simply have to be studied by changing a and the difficult question is where the asymptotic a^2 behavior sets in. From then on a factor 2 variation in a^2 (or better more) is acceptable. We have included our rough estimate where a^2 scaling sets in. Together with the required $L \geq 2.5 \text{ fm} \dots 5 \text{ fm}$, this shows that L/a has to be prohibitively large when the b-quark is simulated as a relativistic quark³, while for

¹ We use the symbol m_h generically when the precise definition of the renormalized mass does not matter.

² At this stage we are interested mostly in the theory and less the phenomenology, where one may ask whether the charm quark is to be treated as a light quark or a heavy one. Top quarks on the other hand are not considered at all. They are heavy enough to safely be considered as decoupled.

³ We should mention that not everybody in the field agrees with this statement. There are lattice QCD computations with quark masses very close to the physical b-quark mass and $am_h \lesssim 1$. Discretisation errors are fitted with polynomials in the lattice spacing and these representations of the data are used to extrapolate the results to the continuum and the physical mass. As an example we cite [12].

source of errors	cases	asymptotics	% effects	References
finite volume effect due to particle exchange around the periodic space		$O(\exp(-m_{\text{gap}}L))$	$m_\pi L \approx 4$	[6, 7, 8]
discretisation errors ($O(a)$ -improved)	lattice QCD with b	$O((aE_i)^2),$ $E_i \sim m_\pi \dots m_B$	extrapolation with $a \leq 0.025 \text{ fm}$	[9, 10, 11]
	lattice HQET without c	$O((aE_i)^2),$ $E_i \sim m_\pi \dots \mathbf{p}_i , \Lambda$	extrapolation with $a \leq 0.1 \text{ fm}$	[9, 10, 11]

Table 1: Effects in lattice QCD computations due to infrared and ultraviolet cutoffs. The lowest particle mass is denoted by m_{gap} ; in QCD with light quarks this is $m_{\text{gap}} = m_\pi$. In the column titled “% effects” we list the condition needed to have systematic errors around the 1% level.

HQET lattices of size $L/a = 32 \dots 64$ seem sufficient. For this reason lattice HQET is a very attractive phenomenological tool.

1.3. Defining effective field theories beyond perturbation theory

We now describe the general concept and formulation of an effective field theory. The special features of HQET will be mentioned in the following subsection. We consider processes in a fundamental theory (QCD or the standard model of particle physics – the important feature is the renormalizability of the theory) at low energy. In particular we first focus on processes (scattering, decay) of particles with masses of this low energy or below it (in HQET also the large mass particles *are* involved as will be discussed soon). In this situation, vacuum fluctuations involving much heavier particles are suppressed and a true creation of the heavier particles is energetically forbidden. One therefore expects to be able to describe the physics of these low energy processes by an effective field theory containing only the fields of the light particles [13]. The leading order Lagrangian of the theory is formed first from the free field theory Lagrangians and all the renormalizable interactions. Assuming the usual power counting, all local composite fields with mass dimension smaller or equal to four are allowed. Let us denote the Lagrangian by \mathcal{L}^{LO} and the Euclidean action is $S^{\text{LO}} = \int d^4x \mathcal{L}^{\text{LO}}(x)$. Correlation functions are then defined by the standard path integral

$$\langle O \rangle_{\text{LO}} = \frac{1}{Z_{\text{LO}}} \int_{\text{fields}} e^{-S^{\text{LO}}} O. \quad (5)$$

with $\langle 1 \rangle_{\text{LO}} = 1$ and O some multilocal product of fields such as $O = \Phi(x)\Phi(y)$. In this way we start with a *renormalizable* theory. For a lattice formulation this means that the *continuum limit* of the theory exists when a finite number of renormalized parameters are kept fixed.

The continuum limit is then also expected to be universal, i.e. independent of the specific discretisation.

Higher order terms in the expansion of physical amplitudes (or correlation functions) in $1/m_h$ are given by including fields with higher mass dimension, which is compensated by the appropriate factor of the large mass in the denominator,

$$\mathcal{L}^{\text{NLO}} = \sum_i \omega_i \mathcal{O}_i, \quad \omega_i = \frac{1}{m_h} \tilde{\omega}_i \quad (6)$$

where the parameters $\tilde{\omega}_i$ are dimensionless. The fields contained in the (multi-local) O are expanded in the same way as the action, $O_{\text{eff}} = O_{\text{LO}} + O_{\text{NLO}} + \dots$. We now have to deal with interactions in eq. (6) which are not renormalizable (by power counting). However, we are only interested in the expansion $\Phi = \Phi_{\text{eff}}^{\text{LO}} + \Phi_{\text{eff}}^{\text{NLO}} + \dots$ of observables Φ in m_h^{-1} . It is therefore sufficient to define the theory with the weight in the path integral expanded, $e^{-S} \rightarrow e^{-S^{\text{LO}}} \{1 - S^{\text{NLO}} + \dots\}$. At NLO accuracy the expansion is then given by

$$\Phi_{\text{eff}}^{\text{LO}} = \langle O^{\text{LO}} \rangle_{\text{LO}} \quad (7)$$

$$\begin{aligned} \Phi_{\text{eff}}^{\text{NLO}} &= \langle O^{\text{NLO}} \rangle_{\text{LO}} \\ &\quad - \left(\langle O^{\text{LO}} S^{\text{NLO}} \rangle_{\text{LO}} - \langle O^{\text{LO}} \rangle_{\text{LO}} \langle S^{\text{NLO}} \rangle_{\text{LO}} \right) \end{aligned} \quad (8)$$

and $S^{\text{NLO}} = \int d^4x \mathcal{L}^{\text{NLO}}(x)$. The term $\Phi_{\text{eff}}^{\text{NLO}}$ (but not the individual terms on the r.h.s. of eq. (8)) is renormalizable with a finite number of counter terms which are equivalent to renormalizing the parameters ω_i (including the LO ones). Also parameters in the fields O are part of the list of ω_i . The reader may worry about divergences in the form of contact terms between \mathcal{L}^{NLO} and O^{LO} in $\langle O^{\text{LO}} S^{\text{NLO}} \rangle_{\text{LO}}$. These, however, can all be absorbed into the ω_i , see [14] and [5].

Renormalizability is particularly important for a non-perturbative evaluation of the path integral in a lattice formulation. The continuum limit of an effective theory

only exists when we treat the higher dimensional interactions as insertions in correlation functions in the form of eq. (8).

1.4. HQET

HQET reaches somewhat beyond the situation discussed above. The difference is that we are interested in processes which do involve the heavy quark h at small momenta (remember we choose the rest frame properly). It is therefore not immediately clear, what are the degrees of freedom to be kept at low energy: what is the complete basis of low energy fields? The answer to this question was found in various ways. We here sketch one line of reasoning.

For smooth fields, the Dirac Lagrangian

$$\mathcal{L} = \bar{\psi}(m_h + D_\mu \gamma_\mu) \psi \quad (9)$$

can be split order by order in $1/m_h$ into decoupled upper and lower component quark field contributions, corresponding to the particle and the anti-particle field:

$$\mathcal{L} = \mathcal{L}_h^{\text{stat}} + \mathcal{L}_h^{(1)} \quad (10)$$

$$+ \mathcal{L}_{\bar{h}}^{\text{stat}} + \mathcal{L}_{\bar{h}}^{(1)} + \mathcal{O}\left(\frac{1}{m_h^2}\right) \quad (11)$$

$$\mathcal{L}_h^{\text{stat}} = \bar{\psi}_h(m_h + D_0) \psi_h, \quad (12)$$

$$\mathcal{L}_{\bar{h}}^{\text{stat}} = \bar{\psi}_{\bar{h}}(m_h - D_0) \psi_{\bar{h}}, \quad (13)$$

$$\mathcal{L}_h^{(1)} = -\frac{1}{2m_h} (O_{\text{kin}} + O_{\text{spin}}). \quad (14)$$

The expansion is correct up to terms of order $1/m_h^2$, assuming $D_0 \psi = \mathcal{O}(m_h)$, $D_k \psi = \mathcal{O}(1) = G_\mu$. Here G_μ is the gauge field, D_μ the covariant derivative and we introduced the higher dimensional fields

$$O_{\text{kin}}(x) = \bar{\psi}_h(x) \mathbf{D}^2 \psi_h(x), \quad (15)$$

$$O_{\text{spin}}(x) = \bar{\psi}_h(x) \boldsymbol{\sigma} \cdot \mathbf{B}(x) \psi_h(x), \quad (16)$$

with

$$\sigma_k = \frac{1}{2} \epsilon_{ijk} \sigma_{ij}, \quad B_k = i \frac{1}{2} \epsilon_{ijk} [D_i, D_j]. \quad (17)$$

The decoupling of the fields $\psi_h, \psi_{\bar{h}}$ is achieved by a Fouldy Wouthuysen-Tani (FTW) transformation (see [15, 16]) of the form

$$\chi = \exp(i\Sigma(m)) \psi, \quad (18)$$

with

$$\Sigma(m) = \frac{-i}{2m_h} D_k \gamma_k + \frac{-i}{4m_h^2} \gamma_k \gamma_0 [D_k, D_0], \quad (19)$$

followed by a projection onto decoupled components

$$\psi_h = P_+ \chi, \quad \psi_{\bar{h}} = P_- \chi, \quad (20)$$

with

$$P_\pm = \frac{1}{2}(1 \pm \gamma_0), \quad P_+ P_- = 0. \quad (21)$$

Analogous expressions for $\bar{\psi}_h$ and $\mathcal{L}_h^{(1)}$ are skipped here. Indeed, in the following we do not consider processes involving the anti-quark field, $\psi_{\bar{h}}$, and therefore drop all terms containing it.

It is worth summarizing some issues that arise in this formal derivation.

- Assuming $D_k = \mathcal{O}(1) = G_\mu$ means that this is a classical derivation: in the quantum field theory path integral we integrate over rough fields, i.e. there are arbitrarily large derivatives. The renormalization of the derived classical Lagrangian could then in principle result in additional terms of a different structure.
- The derivation is perturbative in $1/m_h$, order by order. This is all we want for an EFT. In this way we expect to obtain the *asymptotic* expansion in powers of $1/m_h$.
- There are other ways to “derive” the form of the Lagrangian. One may integrate out the components $P_- \psi, \bar{\psi} P_-$ in a path integral and then perform a formal expansion of the resulting non-local action for the remaining fields in terms of a series of local operators [17]. Or one may perform a hopping parameter expansion of the Wilson-Dirac lattice propagator. The leading term gives the propagator of the static action.

1.5. Heavy quark symmetries

The lowest order Lagrangian $\mathcal{L}_h^{\text{stat}}$ has new symmetries. At each space-time point one may perform $\text{SU}(2)$ rotations in the two-dimensional space spanned by the two (non-relativistic) Dirac-components. This invariance is the spin-symmetry, which for example exactly relates the correlation function of the vector current $V_k^{\text{stat}} = \bar{\psi}_u \gamma_k \psi_h$ to those of the time component of the axial current $A_0^{\text{stat}} = \bar{\psi}_u \gamma_5 \gamma_0 \psi_h$. Furthermore, a phase-transformation $\psi_h(x) \rightarrow e^{i\alpha(\mathbf{x})} \psi_h(x)$ leaves the LO action invariant. It means that the number of h -quarks is *conserved locally* at each space point. It is common to remove the mass term $m_h \bar{\psi}_h \psi_h$ from the Lagrangian. In Minkowski space this can be done by a time-dependent phase transformation of the quark fields. In the Euclidean it turns into an exponential factor. The physical

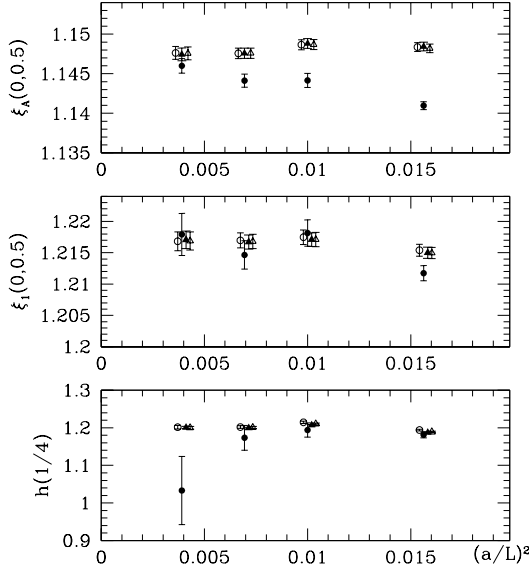


Figure 1: The lattice spacing dependence of $\xi_A(0,0.5)$, $\xi_1(0,0.5)$ and $h(1/4)$ in the quenched approximation [18]. Some data points have been shifted in a^2 for visibility. Different symbols refer to different discretisations of the static action with filled circles the original one by Eichten and Hill [19]. Graph from [18].

interpretation is (in both cases) that one just shifts the energies of the states with a single h -quark by exactly m_h . We find it simpler to keep $m_h \bar{\psi}_h \psi_h$ because a term of this form appears upon renormalization anyway. The formulation without the mass-term, however, exposes another symmetry, namely heavy-quark flavor symmetry which is present when more than one heavy quark are present. It has approximate phenomenological consequences. We do not need it here, mainly since in Nature there is no obvious partner of the b -quark which is heavy enough and forms bound states.⁴

1.6. Theoretical status

In section 1.3 we have emphasized the importance of the renormalizability of the lowest order of the effective theory. In HQET we depend on the renormalizability of the static theory. To our knowledge, this important property of the theory has not been proven to all orders in the coupling constant expansion – in contrast to QCD. Simple power counting does not apply, since the static propagator does not fall off in all directions in momentum space. An alternative strategy is to prove the renormalizability after integrating out the

static quark fields. The resulting non-local observables are then defined in QCD and are closely related to Wilson loops whose renormalizability has been proven to all orders [20, 21, 22, 23, 24]. Indeed, in [24] also observables are considered which are very closely related to the non-local observables resulting from HQET. Furthermore, a significant number of loop computations have been performed, partially to a high order [25]. No problem with the assumed renormalizability has been found. Also the continuum limit of the lattice theory has been studied in quite some detail (see e.g. [18]). Its existence is a non-perturbative “proof” of renormalizability. We use quotation marks, since it is a numerical proof only. Still, the quality of the numerical investigation is very good. We demonstrate it by a graph from [18]. It shows three quantities in the static effective theory, which can be computed precisely. They are constructed from correlation functions in a finite volume with Schrödinger functional boundary conditions [26, 27, 28] i.e. Dirichlet boundary conditions in time, and periodic boundary conditions in space. For the quark fields, the spatial boundary conditions involve a phase θ via,

$$\psi(x + L\hat{k}) = e^{i\theta} \psi(x), \quad (22)$$

$$\bar{\psi}(x + L\hat{k}) = e^{-i\theta} \bar{\psi}(x). \quad (23)$$

Such boundary conditions are (precisely speaking at lowest order in perturbation theory) equivalent to raising the lowest momentum of the finite volume modes from $\mathbf{p} = 0$ to $\mathbf{p} = \mathbf{p}_\theta \equiv \theta \times (1, 1, 1)$ for the quarks and $\mathbf{p} = -\mathbf{p}_\theta$ for the anti-quarks. One can then consider various types of correlation functions, see also section 4. Here we need $f_{A_0}^{\text{stat}}(\theta)$, where a relativistic quark with $\mathbf{p} = \mathbf{p}_\theta$ and a static antiquark with $\mathbf{p} = -\mathbf{p}_\theta$ are created at time zero and are annihilated in the middle of the $T \times L^3$ space-time through the static-light axial current A_0^{stat} . This correlation function is depicted on the left side of figure 4. Forming $\xi_A = f_{A_0}^{\text{stat}}(\theta)/f_{A_0}^{\text{stat}}(\theta')$ gives a first observable, which according to our naive application of dimensional counting and symmetries needs no renormalization. It is also precisely computable. For $\theta = 0, \theta' = 1/2$ it is shown on the top of figure 1. Letting the quark and the static anti-quark propagate from the boundary at $x_0 = 0$ to $x_0 = T$, defines F_1 (rightmost graph in figure 4) and ξ_1 . Its continuum limit is shown for the same kinematics in the middle graph of figure 1. Finally, the ratio h shown at the bottom of figure 1 is constructed from the boundary-to-boundary correlation function of a static quark-antiquark pair. For all three cases, the lattice spacing dependence is shown for four different discretizations. One can see by eye that they

⁴Of course, one often considers the charm quark in an HQET expansion, but on the quantitative level large corrections have to be expected with a mass of around a GeV.

tend to agree at $a = 0$. We have good numerical evidence for the expected renormalizability of the theory. Much more such evidence was seen in later works.

In summary, we have no doubt about the renormalizability of the theory.

1.7. HQET parameters

EFTs have a number of free parameters, the ω_i mentioned above. The number of parameters usually grows rapidly as one increases the order of the expansion. Concerning HQET, we provide an overview for the first two non-trivial orders in table 2. Depending on the application, i.e. the particular observable which is being expanded, the number of parameters which actually contribute may vary significantly. For example in the first row of the table there are three parameters for the Lagrangian at NLO. These generically contribute to any observable, but there are exceptions. For example the splitting of two levels related by the spin symmetry of the theory (an exact symmetry at the static order) depends on a single parameter only, ω_{spin} . And for the computation of the spectrum of the theory, only the first row is needed anyway, since the other rows arise from the expansion of specific local fields.

In general the growth of the numbers of parameters with the order is problematic for phenomenological applications of EFTs. They are usually fixed from experiments, limiting the predictivity enormously. For HQET the situation is actually worse than e.g. for chiral perturbation theory (see [29] and references therein for a recent review). Even when the parameters ω_i are known, the observables cannot be determined by perturbation theory in the couplings (not to be confused with the expansion in $1/m_h$): they are non-perturbative in the QCD coupling irrespective of the order in $1/m_h$. A lattice QCD formulation is needed. In its absence the predictions of the effective theory comprise of approximate scaling (with powers of the quark mass) of certain results from charm to bottom and there are relations between matrix elements due to the enhanced symmetry of the static limit. Instead, with a lattice formulation, the theory becomes fully predictive.

Once one has the lattice formulation, it is also natural to solve the problem of the number of parameters by determining them from lattice-accessible quantities instead of from experimental ones. This is indeed possible. Starting from the general idea [30] a detailed strategy was developed in a number of works which we will discuss in the following. The basic procedure is just to require

$$\Phi_i^{\text{HQET}} = \Phi_i^{\text{QCD}}, \quad i = 1, \dots, N_\omega, \quad (24)$$

for a number of observables equal to the number N_ω of parameters ω_i present at a certain order. This procedure is referred to as matching. The Φ_i do not need to be experimental observables. It suffices that they are accessible to precise lattice simulations.

2. Matching and mass scaling

As simple as it is in principle, there are important issues to be considered and to be understood when eq. (24) is applied in practice.

1. Observables have to be chosen such that the accuracy of the HQET expansion is not compromised: energies have to be sufficiently small. There is, however, no point in going significantly below $\Lambda \approx 400\text{MeV}$, since this scale is always present.
2. The right hand side of eq. (24) has to be computable in lattice QCD, which means that $am_h \ll 1$ has to be reachable.
3. When eq. (24) is implemented non-perturbatively, it has to be imposed at a finite (the desired) quark mass. Since the left side is an approximation, truncated at a given order, the effective theory parameters then do depend on the matching condition imposed.
4. The observables Φ_i have to have a good statistical precision in lattice computations, both in QCD and in HQET.

Clearly item 2. is in conflict with section 1.2, where we explained that $am_h \ll 1$ cannot be reached for large enough volumes where finite size effects are small. This is avoided by having a smaller gap between infrared and ultraviolet cutoff, defining the observables Φ_i in a small volume. Item 1 suggests that the infrared momentum cutoff should be chosen around Λ , namely $L = O(1/\Lambda) = O(\frac{1}{2}\text{fm})$.

2.1. One-loop perturbation theory

Before coming to a general discussion, it is instructive to look at the simplest case of matching in perturbation theory. We consider the static effective theory. Its Lagrangian

$$\mathcal{L}_h^{\text{stat}} = \bar{\psi}_h(m_h^{\text{bare}} + D_0)\psi_h, \quad (25)$$

contains a single parameter, m_h^{bare} . In comparison to eq. (12) we have added a label ‘bare’ to indicate the bare mass parameter. ψ_h etc are the bare fields in the regularized path integral. The explicit form of the heavy quark propagator, which we give later in eq. (84), shows that m_h^{bare} drops out of all observables (at LO) except for the

static (LO)		O(1/m _h) (NLO)		origin	application
Number	ω_i	Number	ω_i		
1	m_{bare}	2	$\omega_{\text{kin}}, \omega_{\text{spin}}$	$\mathcal{L}^{\text{HQET}}$	all
1	$\ln Z_{A_0}^{\text{HQET}}$	2	$c_{A_{0,1}}, c_{A_{0,2}}$	A_0^{HQET}	$B \rightarrow \ell \nu$: f_B , $B_s \rightarrow \ell \bar{\ell}$: f_{B_s}
1		4		A_k^{HQET}	
1		2		V_0^{HQET}	$B \rightarrow \ell \nu \pi$: form-factors f_+, f_0
1		4		V_k^{HQET}	$B \rightarrow \ell \nu \pi$: form-factors f_+, f_0

Table 2: The number of free parameters in HQET at a given order, the specific fields where they appear (“origin”) as well as some examples for applications where they contribute.

relation between the QCD quark mass and one energy level in the static theory, say the mass of the B-meson. All energy differences and all properly normalized⁵ matrix elements are independent of $m_{\text{h}}^{\text{bare}}$.

Interesting, non-trivial, matching happens for composite fields. We choose here the time-component of the axial current,

$$A_{0R}(x) = Z_A A_0, \quad A_0 = \bar{\psi}_u(x) \gamma_5 \gamma_0 \psi_b(x). \quad (26)$$

To distinguish it from the HQET field we label the heavy quark in QCD by b. The matrix element,

$$\langle 0 | A_0^R(\mathbf{x} = 0) | B(\mathbf{p} = 0) \rangle = m_B^{1/2} f_B, \quad (27)$$

of the associated Hilbert space operator defines the decay constant f_B , the only hadronic parameter determining the decay rate $B \rightarrow \ell \nu$. For matching, it is natural to consider more general matrix elements

$$\mathcal{M}_{\text{QCD}}(L, m_b) = \langle \Omega(L) | A_0^R(\mathbf{x} = 0) | B(L) \rangle, \quad (28)$$

to define a suitable quantity Φ_i (i fixed) in eq. (24). In physical processes, L is an inverse momentum scale, but we will later use states in a finite periodic $L \times L \times L$ torus. The state $B(L)$ has the quantum numbers of a B-meson, while $\Omega(L)$ has vacuum quantum numbers.

In generic regularizations, e.g. in dimensional or the Wilson lattice one, the axial current is affected by a non-trivial renormalization $A_{\mu,R} = Z_A A_\mu$. When the renormalization factor Z_A is defined such that the current satisfies the chiral Ward identities [31, 32], eq. (27) gives correctly the weak decay amplitude and thus f_B . The current is then also scale independent.

⁵ A proper mass-independent non-relativistic normalization has to be chosen. The standard one is $\langle B(\mathbf{p}') | B(\mathbf{p}) \rangle = 2(2\pi)^3 \delta(\mathbf{p} - \mathbf{p}')$.

For the moment the relevant property of the states $|\Omega(L)\rangle$ and $|B(L)\rangle$ is that L is the only scale apart from m_b and Λ . Then, for sufficiently small L , the relevant QCD coupling is small and there is a perturbative expansion

$$\mathcal{M}_{\text{QCD}}(L, m_b) = \mathcal{M}^{(0)} + \mathcal{M}_{\text{QCD}}^{(1)}(z) g^2 + \mathcal{O}(g^4) + \mathcal{O}(1/z), \quad z = L m_b. \quad (29)$$

in terms of renormalized coupling and mass $g = \bar{g}, m_b$. We will specify their renormalization scheme and scale when it becomes relevant. For any finite L and m_b , the matrix elements are finite, but the large mass limit, $m_b \rightarrow \infty$ with L fixed does not exist. It is logarithmically divergent [33, 34],

$$\mathcal{M}_{\text{QCD}}^{(1)}(z) \xrightarrow{m_b \rightarrow \infty} (-\gamma_0 \log(z) + B_{\text{QCD}}) \mathcal{M}^{(0)}, \quad (30)$$

$$\gamma_0 = -1/(4\pi^2). \quad (31)$$

This behavior has to be reproduced by the effective theory. As a first step, the bare static-light current

$$A_0^{\text{stat}}(x) = \bar{\psi}_u(x) \gamma_5 \gamma_0 \psi_b(x), \quad (32)$$

is just form-identical to the relativistic one. For the classical current this follows from the FTW transformation and beyond we just observe that there are no other dimension three (or lower) composite fields with the same quantum numbers.

Unlike the relativistic current, there are no chiral Ward identities which fix its renormalization. As a consequence the renormalized current is scale dependent. For example in the lattice regularization we can renor-

malize it by lattice minimal subtraction,⁶

$$A_0^{\text{stat,lat}}(x; \mu) = Z_A^{\text{stat,lat}}(\mu a, g_0) A_0^{\text{stat}}(x), \quad (34)$$

$$Z_A^{\text{stat,lat}} = 1 - \gamma_0 \log(a\mu) g_0^2 + \mathcal{O}(g_0^4). \quad (35)$$

Here a is the lattice spacing, g_0 is the bare coupling and μ is the renormalization scale.

The lowest order anomalous dimension γ_0 coincides with γ_0 from the mass-scaling defined above. The matrix elements

$$\mathcal{M}_{\text{stat}}^{\text{lat}}(L, \mu) = \langle \Omega(L) | Z_A^{\text{stat,lat}} \mathbb{A}_0^{\text{stat}} | B(L) \rangle, \quad (36)$$

corresponding to the above QCD ones have an expansion in the renormalized coupling,

$$\mathcal{M}_{\text{stat}}^{\text{lat}}(L, \mu) = \mathcal{M}^{(0)} + \mathcal{M}_{\text{stat}}^{(1)}(\mu L) g^2 + \mathcal{O}(g^4), \quad (37)$$

$$\mathcal{M}_{\text{stat}}^{(1)}(\mu L) = (-\gamma_0 \log(\mu L) + B_{\text{lat}}) \mathcal{M}^{(0)}. \quad (38)$$

For convenience we put the asymptotic QCD expression and the static one together (up to $\mathcal{O}(g^4, 1/z)$),

$$\begin{aligned} \mathcal{M}_{\text{QCD}} &= (1 + (-\gamma_0 \log(m_b L) + B_{\text{QCD}}) g^2) \mathcal{M}^{(0)}, \\ \mathcal{M}_{\text{stat}}^{\text{lat}} &= (1 + (-\gamma_0 \log(\mu L) + B_{\text{lat}}) g^2) \mathcal{M}^{(0)}. \end{aligned} \quad (39)$$

In this way one sees immediately that a finite renormalization of the static current

$$A_0^{\text{stat,match}}(x; m_b) = \tilde{C}_{\text{match}}(m_b, \mu) A_0^{\text{stat,lat}}(x; \mu), \quad (40)$$

$$\tilde{C}_{\text{match}} = 1 + c_1(\mu/m_b) g^2 + \mathcal{O}(g^4), \quad (41)$$

$$c_1(\mu/m_b) = \gamma_0 \log(\mu/m_b) + (B_{\text{QCD}} - B_{\text{lat}}),$$

brings QCD and the static effective theory into agreement,

$$\begin{aligned} \mathcal{M}_{\text{QCD}} &= \tilde{C}_{\text{match}} \mathcal{M}_{\text{stat}}^{\text{lat}} + \mathcal{O}(1/z) \\ &= \langle \Omega(L) | \mathbb{A}_0^{\text{stat,match}} | B(L) \rangle_{\text{stat}} + \mathcal{O}(1/z). \end{aligned} \quad (42)$$

We emphasise the general structure and the important features of the example.

- The coefficient of the logarithm in eq. (30) and the anomalous dimension of the current in the static theory, eq. (35), match. This matching cannot be enforced, it is a property of the two theories. And it is one of the conditions for the effective theory to describe the asymptotics of QCD.

⁶ For comparison, the renormalization factor of the relativistic lattice current is

$$Z_A = 1 + Z_A^{(1)} g_0^2 + \dots \quad (33)$$

with a pure number (no renormalization scale dependence) $Z_A^{(1)}$, which can be chosen such that the chiral Ward identities hold.

- The relative one-loop coefficient [35, 36],

$$B_{\text{QCD}} - B_{\text{lat}} = -0.137(1), \quad (43)$$

is independent of the external states. They were chosen from two rather different classes in the two cited references. Again this is a necessary condition for the effective theory to describe QCD.

- Both $\mathcal{M}^{(0)}$ and B_{QCD} do depend on the external states. Let us label a matrix element for a different pair of states by just a prime. In ratios of these matrix elements,

$$\mathcal{R}_{\text{QCD}} = \mathcal{M}'_{\text{QCD}} / \mathcal{M}_{\text{QCD}}, \quad (44)$$

the entire renormalization and matching of the current drops out, since it is multiplicative. One then has effective theory predictions

$$\mathcal{R}_{\text{QCD}} = \mathcal{R}_{\text{stat}} + \mathcal{O}(1/z) \quad (45)$$

$$\mathcal{R}_{\text{stat}} = \mathcal{R}_{\text{stat}}^{(0)} + \mathcal{R}_{\text{stat}}^{(1)} g^2 + \mathcal{O}(g^4), \quad (46)$$

$$\mathcal{R}_{\text{stat}}^{(0)} = (\mathcal{M}'_{\text{stat}})^{(0)} / \mathcal{M}_{\text{stat}}^{(0)}, \quad (47)$$

$$\begin{aligned} \mathcal{R}_{\text{stat}}^{(1)} &= \frac{(\mathcal{M}'_{\text{stat}})^{(1)}}{(\mathcal{M}'_{\text{stat}})^{(0)}} - \frac{(\mathcal{M}_{\text{stat}})^{(1)}}{(\mathcal{M}_{\text{stat}})^{(0)}} \\ &= B'_{\text{lat}} - B_{\text{lat}} = B'_{\text{QCD}} - B_{\text{QCD}}. \end{aligned} \quad (48)$$

- The particular number of eq. (43) depends on the renormalization scheme for the static current. Here we chose minimal subtraction, a scheme which is not independent of the regularization. Therefore, $B_{\text{QCD}} - B_{\text{lat}}$ depends on the details of the regularization chosen in [35, 36]. It is valid for the $\mathcal{O}(a)$ improved Wilson lattice regularization.
- Of course the matrix elements of the matched static current in eq. (42) do not depend on any details of the regularization. Their finite renormalization has been chosen to match QCD. This is unique. In eq. (42) we did not indicate the one-loop nature. Indeed, we expect this equation to hold to all orders in the coupling and also beyond, non-perturbatively.
- We have nowhere given the renormalization scale/scheme for coupling and mass. At the one-loop order all expressions are independent of it. The scheme only matters for the renormalization factor of the current itself. In the following section we will also discuss a convenient choice of renormalization scales.

2.2. Higher orders in the coupling and renormalization group invariants

In this section we explain on the one hand what is known at higher orders in the coupling and on the other hand, how one passes to renormalization group invariants, which are independent of schemes and scales. In particular they allow for a clean factorization of observables into a non-perturbative matrix element and a multiplicative matching function, which has a perturbative expansion. This separation makes efficient use of the high order perturbative information accumulated over the years [33, 34, 37, 38, 39, 40, 41, 42, 43, 44, 45]. We note, however, that we only know how to apply this strategy to the lowest order, static, effective theory. A hurried reader may therefore skip this section and proceed to the following one.

2.2.1. RG functions and invariants

It is well known, that fixed order perturbation theory, where all observables are expressed in terms of a renormalized coupling and masses at one fixed renormalization scale is not the best choice. In fact, if scales rather different from the renormalization scale are relevant in the observables, large logarithms multiplying powers of the coupling are present and the accuracy of perturbation theory is not good. This is a reason to consider running coupling and mass, i.e. coupling and mass as functions of the renormalization scale,

$$\bar{g}(\mu), \bar{m}_i(\mu), \quad (49)$$

and the associated renormalization group equations (RGE). Here i runs over the different flavors and all masses are defined in QCD, also the mass of the quark treated by HQET. A consequent application of the RGEs is to use their solutions and express all observables in terms of renormalization group invariants.

Here we do not give an introduction to the RG but just recommend Ref. [46]. We mainly describe the relevant formulae in order to apply them to our matching

problem. We work in an unspecified massless renormalization scheme, where the renormalization factors do not depend on the masses. Consequently the renormalization group functions do not depend on the masses. Examples of massless schemes are (modified) minimal subtraction in dimensional regularization (MS, $\overline{\text{MS}}$) or lattice regularization (lat) or a Schrödinger functional scheme (SF) [26, 47]. The latter is independent of the regularization.

Our renormalization group (RG) functions are defined through

$$\mu \frac{\partial \bar{g}}{\partial \mu} = \beta(\bar{g}), \quad \frac{\mu}{\bar{m}_i} \frac{\partial \bar{m}_i}{\partial \mu} = \tau(\bar{g}), \quad (50)$$

$$\frac{\mu}{\mathcal{M}_{\text{stat}}^s} \frac{\partial \mathcal{M}_{\text{stat}}^s}{\partial \mu} = \gamma(\bar{g}). \quad (51)$$

Apart from the running coupling and running quark mass we here consider the matrix element $\mathcal{M}_{\text{stat}}^s$ of a (multiplicatively renormalizable) composite field renormalized at scale μ . We label it with a superscript s for the scheme to remain consistent with previous notation. One may identify it with eq. (36), but other matrix elements of general composite operators are possible as well. The RG functions have asymptotic expansions

$$\beta(\bar{g}) \stackrel{\bar{g} \rightarrow 0}{\sim} -\bar{g}^3 \left\{ b_0 + \bar{g}^2 b_1 + \dots \right\}, \quad (52)$$

$$b_0 = \frac{1}{(4\pi)^2} \left(11 - \frac{2}{3} N_f \right) \\ b_1 = \frac{1}{(4\pi)^4} \left(102 - \frac{38}{3} N_f \right), \quad (53)$$

$$\tau(\bar{g}) \stackrel{\bar{g} \rightarrow 0}{\sim} -\bar{g}^2 \left\{ d_0 + \bar{g}^2 d_1 + \dots \right\}, \quad (54)$$

$$d_0 = 8/(4\pi)^2, \quad (55)$$

$$\gamma(\bar{g}) \stackrel{\bar{g} \rightarrow 0}{\sim} -\bar{g}^2 \left\{ \gamma_0 + \bar{g}^2 \gamma_1 + \dots \right\}. \quad (56)$$

The integration constants of the solutions to the RGE define the RG invariants

$$\Lambda = \varphi_g(\bar{g}) \mu = \mu \left(b_0 \bar{g}^2 \right)^{-b_1/(2b_0^2)} e^{-1/(2b_0 \bar{g}^2)} \exp \left\{ - \int_0^{\bar{g}} dx \left[\frac{1}{\beta(x)} + \frac{1}{b_0 x^3} - \frac{b_1}{b_0^2 x} \right] \right\}, \\ M_i = \varphi_m(\bar{g}) \bar{m}_i = \bar{m}_i (2b_0 \bar{g}^2)^{-d_0/2b_0} \exp \left\{ - \int_0^{\bar{g}} dx \left[\frac{\tau(x)}{\beta(x)} - \frac{d_0}{b_0 x} \right] \right\}, \\ \mathcal{M}_{\text{stat}}^{\text{RGI}} = \varphi_{\text{stat}}(\bar{g}) \mathcal{M}_{\text{stat}}^s = \mathcal{M}_{\text{stat}}^s \left[2b_0 \bar{g}^2 \right]^{-\gamma_0/2b_0} \exp \left\{ - \int_0^{\bar{g}} dx \left[\frac{\gamma(x)}{\beta(x)} - \frac{\gamma_0}{b_0 x} \right] \right\}, \quad (57)$$

where $\bar{g} \equiv \bar{g}(\mu)$, $\bar{m}_i \equiv \bar{m}_i(\mu)$, $\mathcal{M}_{\text{stat}}^s \equiv \mathcal{M}_{\text{stat}}^s(\mu)$. There are no corrections to eqs. (57) with exact RG functions. Instead, when we only have access to their perturbative expansions such as eq. (52) there are truncation errors in the functions $\varphi_r(\bar{g})$. For example, in order to obtain a numerical result for Λ given a pair of numbers for $\bar{g}(\mu)$, μ , the integrand [...] in eq. (57) may in principle be expanded as [...] = $c_2 x + c_3 x^3 + \mathcal{O}(x^5)$. Knowing c_2 , the error made is (asymptotically) $\approx c_3 \bar{g}^4/4$ and the same is true when we insert the truncation of $\beta(x)$ and then integrate. When we discuss numbers, we will always expand the RG functions, not the full integrands.

Physical observables can be written as

$$\mathcal{P} = \mathcal{P}(\Lambda, \{M_i\}, \{p_i\}) \quad (58)$$

making it manifest that they do not depend on a renormalization scale μ ,

$$\mu \frac{d}{d\mu} \mathcal{P} = 0. \quad (59)$$

In the following section we express the lowest order HQET approximation of matrix elements \mathcal{M}_{QCD} in this way and define a RGI mass scaling function, which describes the mass-dependence beyond the asymptotic form eq. (3).

2.2.2. Mass scaling

As a first step we choose a suitable renormalization scale,

$$\mu = m_*, \quad (60)$$

where the solution of

$$m_* = \bar{m}(m_*), \quad (61)$$

defines m_* . We further use the shorthand

$$g_* = \bar{g}(m_*). \quad (62)$$

The coupling g_* can be determined for any value of M/Λ by combining the first two equations eq. (57) to

$$\begin{aligned} \frac{\Lambda}{M} &= \frac{\varphi_g(g_*)}{\varphi_m(g_*)} \\ &= \exp \left\{ - \int^{g_*(M/\Lambda)} dx \frac{1 - \tau(x)}{\beta(x)} \right\}. \end{aligned} \quad (63)$$

The solution of this equation defines a function $g_*(M/\Lambda)$.

With the above choices the matching function simplifies to

$$\tilde{C}_{\text{match}}(m_*, m_*) \equiv C_{\text{match}}(g_*) \quad (64)$$

$$= 1 + c_1(1) g_*^2 + \dots, \quad (65)$$

and we have

$$\begin{aligned} \mathcal{M}_{\text{QCD}} &= C_{\text{match}}(g_*) \times \mathcal{M}_{\text{stat}}(\mu) + \mathcal{O}(1/m_h) \\ &= \frac{C_{\text{match}}(g_*)}{\varphi_{\text{stat}}(g_*)} \mathcal{M}_{\text{stat}}^{\text{RGI}} + \mathcal{O}(1/m_h). \end{aligned} \quad (66)$$

The g_* -dependence is equivalently to the mass dependence and defines another RG function γ_{match} ,

$$\gamma_{\text{match}}(g_*) \equiv \frac{m_*}{\mathcal{M}_{\text{QCD}}} \frac{\partial \mathcal{M}_{\text{QCD}}}{\partial m_*} \Big|_{\Lambda}, \quad (67)$$

with asymptotics

$$\gamma_{\text{match}}(g) \stackrel{g \rightarrow 0}{\sim} -\gamma_0 g^2 - \gamma_1^{\text{match}} g^4 + \dots \quad (68)$$

Because the leading order coefficient γ_0 is unchanged, “match” is just another renormalization scheme for the axial current A_0^{stat} . In this scheme, at scale $\mu = m_*$, its matrix elements are equal to the QCD ones up to order $1/m_h$. We therefore refer to it as the matching scheme.

Finally, a complete transition to renormalization group invariants is achieved by changing to the RGI mass scaling function

$$\begin{aligned} \rho_{\text{PS}}(M/\Lambda) &\equiv \frac{M}{\mathcal{M}_{\text{stat}}} \frac{\partial \mathcal{M}_{\text{stat}}}{\partial M} \Big|_{\Lambda} = \frac{M}{C_{\text{PS}}} \frac{\partial C_{\text{PS}}}{\partial M} \Big|_{\Lambda} \\ &= \frac{\gamma_{\text{match}}(g_*)}{1 - \tau(g_*)}, \end{aligned} \quad (69)$$

and to

$$\begin{aligned} \mathcal{M}_{\text{QCD}} &= C_{\text{PS}}(M/\Lambda) \times \mathcal{M}_{\text{stat}}^{\text{RGI}} + \mathcal{O}(1/m_h) \\ C_{\text{PS}}(M/\Lambda) &= C_{\text{match}}(g_*) / \varphi_{\text{stat}}(g_*) \\ &= \exp \left\{ \int^{g_*} dx \frac{\gamma_{\text{match}}(x)}{\beta(x)} \right\}. \end{aligned} \quad (70)$$

Everywhere it is understood that $g_* = g_*(M/\Lambda)$. In the last equation, the integral at the lower bound is to be understood as in eq. (57).

At leading order in $1/m_h$ the conversion function C_{PS} contains the full (logarithmic) mass-dependence, while the non-perturbative effective theory matrix elements, $\mathcal{M}_{\text{stat}}^{\text{RGI}}$, are mass independent numbers.

An interesting application is the asymptotics of the decay constant of a heavy-light pseudo-scalar (e.g. B):⁷

$$F_{\text{PS}} \stackrel{M \rightarrow \infty}{\sim} \frac{[\ln(M/\Lambda)]^{\gamma_0/2b_0}}{\sqrt{m_{\text{PS}}}} \mathcal{M}_{\text{stat}}^{\text{RGI}} \times [1 + \mathcal{O}([\ln(M/\Lambda)]^{-1})]. \quad (71)$$

In perturbation theory, the logarithmic corrections are computed by solving eq. (63) for g_* and then integrating eq. (70).

⁷Note the slow, logarithmic, decrease of the corrections in eq. (71). We will see below, in the discussion of figure 2, that the perturbative evaluation of $C_{\text{PS}}(M_b/\Lambda)$ is somewhat problematic.

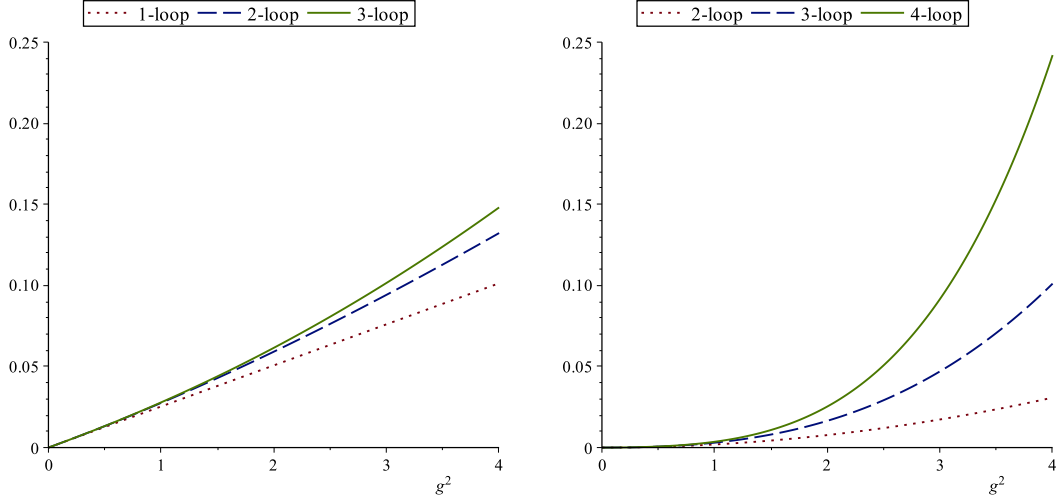


Figure 2: The function $\gamma_{\text{match}}(g)$ as a function of $g^2 = g_*^2$ for $N_f = 3$ flavors in the $\overline{\text{MS}}$ scheme. On the left we show $\gamma_{\text{match}} = \gamma_{\text{match}}^{A_0}$ for the time component of the axial current, on the right we show the difference $\gamma_{\text{match}}^{V_k} - \gamma_{\text{match}}^{A_0}$. Note that at 1-loop order the latter vanishes.

2.3. On the accuracy of perturbation theory

When one evaluates functions such as C_{PS} in a given order of perturbation theory, various quantities enter such as the beta-function, the quark mass anomalous dimension. Apart from γ_{match} , these all have a well behaved perturbative expansion in the $\overline{\text{MS}}$ scheme, see appendix A.2.2 of [5] for a table of the coefficients. Keeping this in mind, we just discuss γ_{match} . In the left graph in figure 2 we plot different orders of γ_{match} . For the larger values g_*^2 in the plot one may get worried about neglecting higher order terms. Note that g_*^2 is around 2.5 for the b-quark and it is out of the range of the graph for the charm quark.

However, a more serious reason for concern derives from the right hand side graph. There the difference of the anomalous dimensions for V_k and A_0 is shown. For such differences perturbation theory is known to be one loop higher [48] and the perturbative coefficients do grow further. Asymptotic convergence seems to be useful only for rather small couplings or masses far above the b-quark mass. At the b-quark mass every known perturbative order contributes about an equal amount. Since we do not understand the reason for this behavior, it raises concern about using perturbation theory for the matching functions.

Let us emphasize, that the bad behavior is easily traced back to the function C_{match} and was noted in [48]. We tried earlier [5] to rearrange the perturbative series in order to find a more stable perturbative prediction, but we did not succeed.

2.4. Matching at NLO in $1/m_h$

For quantitative phenomenological results one has to compute also $1/m_h$ corrections in HQET. Is it consistent to match perturbatively as we discussed in the previous sections? We saw that the uncertainty due to a truncation of the perturbative matching expressions at l -loop order corresponds to a relative *error*

$$\frac{\Delta(C_{\text{PS}})}{C_{\text{PS}}} = \frac{\Delta(\mathcal{M}_{\text{QCD}})}{\mathcal{M}_{\text{QCD}}} \propto [\bar{g}^2(m_*)]^l \quad (72)$$

$$\sim \left[\frac{1}{2b_0 \ln(m_*/\Lambda_{\text{QCD}})} \right]^l.$$

As m_* is made large, this perturbative error decreases only logarithmically. It becomes dominant over the power correction which one wants to include by pushing the HQET expansion to NLO,

$$\frac{\Delta(C_{\text{PS}})}{C_{\text{PS}}} \xrightarrow{m_* \gg \Lambda} \frac{\Lambda}{m_*}. \quad (73)$$

With a perturbative matching function, one does not perform a consistent NLO expansion such that errors decrease as $1/m_h^2$.

A practically even more serious issue is that at NLO one has to deal with the mixing of operators with lower dimensional ones. For example $O_{\text{kin}} = \bar{\psi}_h \mathbf{D}^2 \psi_h$ mixes with $\bar{\psi}_h D_0 \psi_h$ and $\bar{\psi}_h \psi_h$. In this situation mixing coefficients are power divergent $\sim a^{-n}$. In the example we have $n = 1, 2$. Subtracting power divergences in perturbation theory and then computing the matrix elements non-perturbatively always leaves a divergent re-

mainder. The non-perturbative continuum limit of matrix elements of perturbatively subtracted operators does not exist.

We are lead to conclude that it is necessary to perform matching and renormalization non-perturbatively. The only alternative is to supplement the theory by assumptions. Namely one may assume that at the lattice spacings available in practice, power divergences of the form $g_0^{2l}/(m_b a)^n$ are small since $m_b a > 1$. This then has to be combined with the assumption that the b-quark is not large enough to be in the asymptotic region of eq. (73).

2.5. Non-perturbative matching

2.5.1. Scope

A true non-perturbative matching as in eq. (24) eliminates the problems we just discussed: slow asymptotic convergence of PT, power divergent remainder terms in the subtraction of lower dimensional operators. We do, however, still have to cope with the condition $m_b a \ll 1$ for the computation of Φ_i^{QCD} . Before we explain the strategy to deal with this, we would like to emphasize a point about the magnitude of $1/m_h$ corrections which sometimes leads to confusions.

The size of these corrections does depend on the matching conditions used: after imposing a generic condition, eq. (24), the decay constant of the B-meson once computed at LO and once computed at NLO in $1/m_h$ differ by an amount $\mathcal{O}(1/m_h)$. However, how much this difference is exactly, depends on which set $\{\Phi_i\}$ was chosen for matching the theories. We are free to choose $\Phi_1 = m_B$, $\Phi_2 = \langle 0 | \bar{A}_0^R | B(\mathbf{p} = 0) \rangle$. With this choice, the decay constant of the B-meson is exact at all orders in $1/m_h$.

This rather trivial fact has to be remembered. The exact size of the corrections is only defined, once one has fixed how the matching is performed. What we said before implies that one has to define non-perturbatively how the matching is performed. Only then does the splitting of a HQET result into different orders acquire a precise meaning.

Let us illustrate the consequences on a frequently discussed example, namely the mass formulae

$$m_B^{\text{av}} \equiv \frac{1}{4} [m_B + 3m_{B^*}] \quad (74)$$

$$= m_b + \bar{\Lambda} + \frac{1}{2m_b} \lambda_1 + \mathcal{O}(1/m_b^2) \quad (75)$$

$$\Delta m_B \equiv m_{B^*} - m_B = -\frac{2}{m_b} \lambda_2 + \mathcal{O}(1/m_b^2) \quad (76)$$

with (ignoring renormalization)

$$\lambda_1 = \langle B | O_{\text{kin}} | B \rangle, \quad \lambda_2 = \frac{1}{3} \langle B | O_{\text{spin}} | B \rangle. \quad (77)$$

The quantity $\bar{\Lambda}$ is referred to as “static binding energy” and λ_1 as the kinetic energy of the b-quark inside the B-meson. Also here, depending on how one formulates the matching conditions, one changes $\bar{\Lambda}$ by a term of order Λ_{QCD} . Similarly, the kinetic term $\lambda_1/(2m_b)$ has a non-perturbative matching scheme dependence of order $\Lambda_{\text{QCD}}^2/m_b$ and thus λ_1 itself has a matching scheme dependence of order Λ_{QCD}^2 . In fact we could set $\Phi_1 = m_B^{\text{av}}$. At static order this means $m_b + \bar{\Lambda} = m_B^{\text{av}}$ and at NLO it is eq. (75) without the $\mathcal{O}(1/m_b^2)$ correction. If both are to be valid, one has $\lambda_1 = 0$.

For this reason, our scope is not to compute (and therefore first define) quantities such as $\bar{\Lambda}$ but to compute physical observables such that they are correct up to corrections of order $1/m_h^2$. For this purpose we need to determine the bare parameters ω_i . We do not need to define renormalized ones. We ask the reader to keep in mind that since ω_i are bare parameters, they depend on the bare gauge coupling (equivalently the lattice spacing) and the heavy quark mass, where we may choose the RGI mass, M . Further dependences on the details of the discretisation are kept implicit.

2.5.2. Strategy

The general idea how to satisfy $m_b a \ll 1$ is to perform the matching step in a finite space-time volume of linear dimension $L = L_1$ [30], exactly in line with the idea how to cover the scale hierarchy in the computation of running couplings [50]. Choosing $L_1^{-1} \approx \Lambda$, the HQET expansion of correlation functions at distances $|x| = \mathcal{O}(L_1)$ is valid. $L_1 \approx 0.5 \text{ fm}$ is a reasonable choice. This allows for lattice spacings of $a = 0.02 \text{ fm}$ and significantly smaller. One can then perform continuum extrapolations with several points satisfying $m_b a < 1/2$ and determine

$$\Phi_i^{\text{QCD}}(L_1, M, 0) = \lim_{a \rightarrow 0} \Phi_i^{\text{QCD}}(L_1, M, a), \quad (78)$$

as indicated on the left side of figure 3. One is now free to use the matching condition, eq. (24), to determine the ω_i at a given resolution L_1/a . Explicitly, we write the HQET expansion in a matrix notation

$$\Phi^{\text{HQET}} = \eta + \varphi \omega, \quad (79)$$

with a $N_\omega \times N_\omega$ matrix φ and a homogeneous static part η_i , $i = 1, \dots, N_\omega$. Both η and φ can be computed by numerical simulations of HQET. Solving eq. (79) defines

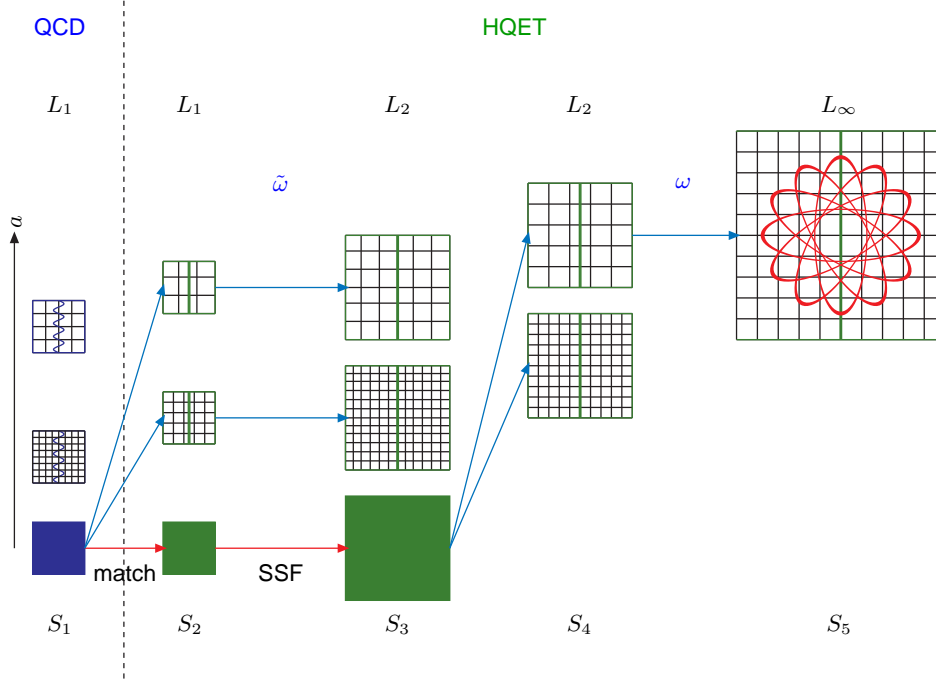


Figure 3: The ALPHA collaboration strategy for matching of QCD and HQET. The bottom row denotes the continuum limit obtained by an extrapolation of the results in each column. Graph from [49].

a first set of HQET parameters

$$\begin{aligned} \tilde{\omega}(M, a) &= \\ \varphi^{-1}(L_1, a) & \left(\Phi^{\text{QCD}}(L_1, M, 0) - \eta(L_1, a) \right). \end{aligned} \quad (80)$$

For reasonable resolutions, say $L/a \geq 8$, where discretisation errors may be assumed to be small, we have $a \leq L_1/8 \approx 0.06$ fm. Remembering that one should always have a range of lattice spacings in order to carry out a continuum extrapolation, we realize that such lattice spacings are still too small to perform the large volume HQET computations to determine the physical energy levels and matrix elements.

For this reason, the full strategy includes a so called step scaling step, to reach the same Φ^{HQET} but for $L = L_2 = 2L_1$:

$$\begin{aligned} \Phi^{\text{HQET}}(L_2, M, 0) &= \\ = \lim_{a \rightarrow 0} & \left[\eta(L_2, a) + \varphi(L_2, a) \tilde{\omega}(M, a) \right]. \end{aligned} \quad (81)$$

This set of observables then serves to determine the desired parameters

$$\begin{aligned} \omega(M, a) &= \\ \varphi^{-1}(L_2, a) & \left(\Phi^{\text{HQET}}(L_2, M, 0) - \eta(L_2, a) \right). \end{aligned} \quad (82)$$

Here lattice spacings can be used which are suitable for large volume HQET computations. The overall strategy is depicted in figure 3. It is explained in more detail in [49].

2.5.3. The electroweak heavy-light currents

For the phenomenological treatment of (semi-) leptonic B-decays in the standard model, one needs both the axial current and the vector current. Our discussion above has to be generalized accordingly. The finite renormalization (for matching) of space and time-components is different, but in a minimal subtraction scheme, all currents have the same anomalous dimension in the static effective theory because they are related by spin symmetry and the chiral symmetry which emerges when the light quarks are massless. Details can be found in [5].

Non-perturbative matching conditions for the full set of currents have been discussed in [51]. They have partially been investigated in perturbation theory [52, 53, 54], see [55] for more details.

3. Discretized HQET

We need a lattice formulation in order to treat HQET beyond perturbation theory in the QCD coupling. The static action discretized on a hyper-cubic lattice is

$$\mathcal{L}_h^{\text{stat}} = \frac{1}{1 + am_h^{\text{bare}}} \bar{\psi}_h(x) [\nabla_0^* + m_h^{\text{bare}}] \psi_h(x), \quad (83)$$

with ∇_μ^* the gauge covariant backward derivative. Compared to the form written down first by Eichten and Hill [19] we just added the mass term. The static propagator in a gauge background is

$$G_h(x, y) = \theta(x_0 - y_0) \delta(\mathbf{x} - \mathbf{y}) e^{-m_h^{\text{bare}}(x_0 - y_0)} \times \mathcal{P}(y, x; 0)^\dagger P_+, \quad (84)$$

$$\text{with } m_h^{\text{bare}} = \frac{1}{a} \ln(1 + am_h^{\text{bare}}), \quad (85)$$

where $\mathcal{P}(x, y; 0)$ parallel transports fields in the fundamental representation from y to x along a time-like path and the lattice θ -function is $\theta(t) = 0$ for $t < 0$ and $\theta(t) = 1$ for $t \geq 0$. It is a simple exercise to obtain eq. (84) from the defining equation

$$\frac{1}{1 + am_h^{\text{bare}}} (\nabla_0^* + m_h^{\text{bare}}) G_h(x, y) = \delta(x - y),$$

where ∇_0^* is the covariant derivative with respect to the argument x . The propagator eq. (84) is valid in any gauge field background and therefore shows that all correlation functions with a static quark have a mass-dependence $C(x) = C(x)|_{m_h^{\text{bare}}=0} \times e^{-m_h^{\text{bare}}|x_0|}$. Equivalently we see that the mass m_h^{bare} in the Lagrangian just yields an energy shift

$$E^{\text{QCD}} = E^{\text{stat}}|_{m_h^{\text{bare}}=0} + m_h^{\text{bare}}. \quad (86)$$

We now briefly discuss the most important features of the discretized static effective theory. The action is (non-perturbatively) $\mathcal{O}(a)$ improved without adding any counter-terms and therefore without tuning any parameters. This is a consequence of the local conservation of the b-quark number and the spin symmetry, which are exactly preserved in the formulation eq. (83) on the lattice [56]. These symmetries do not allow for dimension five fields (containing $\psi_h, \bar{\psi}_h$) in Symanzik's effective Lagrangian describing the discretisation errors. As a consequence energies scale to the continuum with lattice spacing errors proportional to $a^2 \log(a\Lambda)^n$ at small lattice spacing⁸. Improvement terms of the form

$a\delta\mathcal{O}$, $[\delta\mathcal{O}] = 4$ are, however, necessary for fields \mathcal{O} such as $\mathcal{O} = A_0^{\text{stat}}$. For the matrix element determining f_B , there is a single such counter-term [56]. After including it with a properly chosen coefficient, one again has $\mathcal{O}(a^2)$ scaling to the continuum limit.

The above features are very attractive. There is, however, a (numerical, Monte Carlo) issue with the static theory, eq. (83). It has its origin in the fact that

$$E^{\text{stat}}|_{m_h^{\text{bare}}=0} \sim \left(\frac{1}{a} r^{(1)} + \mathcal{O}(a^0) \right) g_0^2 + \mathcal{O}(g_0^4), \quad (87)$$

has a linear divergence (which is then cancelled by $m_h^{\text{bare}} \sim -g_0^2 r^{(1)}/a$ in the physical energies). The numerical value is

$$r^{(1)} = 0.1685 \quad \text{for the action eq. (83)}. \quad (88)$$

The problem is not – as originally was thought – to determine m_h^{bare} non-perturbatively. Rather the statistical errors of, for example, two-point correlation functions of a static B-meson with $m_h^{\text{bare}} = 0$ behave approximately as⁹ [59, 60]

$$\text{stat. error} \stackrel{x_0 \rightarrow \infty}{\sim} \mathcal{A}_N e^{-m_\pi x_0/2} \quad (89)$$

while (at least at small a) the correlation function scales as

$$\text{correlator} \stackrel{x_0 \rightarrow \infty}{\sim} \mathcal{A}_S e^{-E^{\text{stat}} x_0} \sim \mathcal{A}_S e^{-r^{(1)} g_0^2 x_0/a + \dots}. \quad (90)$$

We then have

$$\frac{\text{signal}}{\text{noise}} \sim \frac{\mathcal{A}_S}{\mathcal{A}_N} e^{-[E^{\text{stat}} - m_\pi/2] x_0}, \quad (91)$$

where as before E^{stat} for $m_h^{\text{bare}} = 0$ enters. While methods to use translation invariance with the help of “stochastic sources” [61] can reduce the pre-factor \mathcal{A}_N , the correlators inevitably disappear in the noise at some time $x_0 = \mathcal{O}(a/r^{(1)})$. We here set $g_0 \approx 1$ as appropriate for the considered gauge action. Inserting further that small lattice spacings means $a \leq 0.05\text{fm}$, we see that it is very difficult to have reasonable precision around and beyond one fm distance. However, this is the time separation where one can be confident that the desired ground state dominates. This problem brought progress in the static theory (and therefore in HQET) to a stop in the beginning of the nineties.

Our description of the issue already suggests the solution. The coefficient $r^{(1)}$ is regularization dependent. Acceptable alternative discretizations can be

⁸See [57, 58] for a discussion of the logarithmic modifications.

⁹Remember that we can set $m_h^{\text{bare}} = 0$ due to eq. (86).

found which have much smaller values [18, 62], for example

$$r^{(1)} = 0.0352 \quad \text{for “HYP2” action [18]}. \quad (92)$$

Our previous estimate is now pushed to time separations of around 4 fm. In practice it turns out that the estimate is overly optimistic, since it neglects the finite terms in E^{stat} . The effect of the size of $r^{(1)}$ is also seen in figure 1 where the results with the Eichten Hill action, eq. (83), have much larger statistical errors and these do grow towards the continuum limit, where the time separation in the correlation functions diverges when it is measured in lattice units.

It is interesting to compare the HQET situation (HYP2) to the one for Nucleon matrix elements. The energy difference $E^{\text{stat}} - m_\pi/2$ has to be compared to $m_{\text{nucleon}} - 3m_\pi/2$. At a pion mass of $m_\pi = 350\text{MeV}$ and a lattice with a small lattice spacing, $a = 0.05\text{ fm}$ we compare about 900 MeV for the former to 600 MeV for the nucleon. For HQET this gets (slowly) worse for even smaller lattice spacings and for the nucleon it gets quickly worse towards smaller pion masses. In both cases it is an unpleasant mass scale that governs the time-dependence of the signal-to-noise ratio.

Given that correlation functions at 2-3 fm are not really accessible, one would like to have methods which work reliably at smaller distances. A technique that accelerates the approach of masses and matrix elements to the ground state quantities is the use of correlation function matrices constructed from a few smeared interpolating fields [63, 64]. These correlation functions can be analysed by the “GEVP” method [65, 66, 67] and then a systematic acceleration of the (asymptotic) convergence to the ground state is present. Physically it means that one uses trial wave functions in a variational calculation. The method is easily modified to be applicable also to matrix elements [67, 68] and to effective theories such as HQET. We note that the acceleration of the asymptotic convergence is proven mathematically [67], but it is less clear where asymptotia sets in in practice. The numerical results of section 5 are based on the GEVP technique.

4. Verification of HQET

In a first step in non-perturbative investigations of HQET, it is of considerable interest to verify the mass-scaling of QCD observables predicted by the lowest order effective theory. This can only be done with the help of lattice gauge theory, where we can change the quark masses. As for the matching strategy discussed

above, a natural choice is to focus on observables in a finite volume. For reasons to be explained shortly, Schrödinger functional boundary conditions were chosen with a $T \times L \times L \times L$ geometry, where periodic boundary conditions (up to a phase θ for the quarks, see section 1.6) are present in the $L \times L \times L$ space. Without dynamical fermions the verification was carried out with $L \approx 0.2\text{ fm}$ $T = L$ [69] and with $N_f = 2$ dynamical fermions with $L \approx 0.5\text{ fm}$, $T = L$ [70].

We here focus on $N_f = 2$ observables constructed from the correlation functions

$$f_{A_0}(x_0, \theta) = -\frac{1}{2} \int d^3\mathbf{y} d^3\mathbf{z} \langle A_0(x) \bar{\zeta}_b(\mathbf{y}) \gamma_5 \zeta_l(\mathbf{z}) \rangle, \quad (93)$$

$$k_{\bar{q}}(x_0, \theta) = -\frac{1}{6} \sum_k \int d^3\mathbf{y} d^3\mathbf{z} \langle V_k(x) \bar{\zeta}_b(\mathbf{y}) \gamma_k \zeta_l(\mathbf{z}) \rangle, \quad (94)$$

as well as the boundary-to-boundary correlations

$$F_1 = -\frac{1}{2L^6} \int d^3\mathbf{y} d^3\mathbf{z} d^3\mathbf{y}' d^3\mathbf{z}' \langle \bar{\zeta}'_l(\mathbf{y}') \gamma_5 \zeta'_b(\mathbf{z}') \bar{\zeta}_b(\mathbf{y}) \gamma_5 \zeta_l(\mathbf{z}) \rangle, \quad (95)$$

$$K_1 = -\frac{1}{6L^6} \sum_k \int d^3\mathbf{y} d^3\mathbf{z} d^3\mathbf{y}' d^3\mathbf{z}' \langle \bar{\zeta}'_l(\mathbf{y}') \gamma_k \zeta'_b(\mathbf{z}') \bar{\zeta}_b(\mathbf{y}) \gamma_k \zeta_l(\mathbf{z}) \rangle. \quad (96)$$

They are illustrated in figure 4. Fields $\zeta, \bar{\zeta}$ can be thought of as quark fields at the boundary $x_0 = 0$ while $\zeta', \bar{\zeta}'$ are located at $x_0 = T$. The above correlation functions are gauge invariant despite the different locations of ζ and $\bar{\zeta}$. This is due to the fixed gauge fields at the boundary; it is a very useful feature of the Schrödinger functional which allows for the projection onto quark momenta

$$\mathbf{p} = \mathbf{p}_\theta \equiv (\theta, \theta, \theta)/L \quad (97)$$

in the above correlators (and $\mathbf{p} = -\mathbf{p}_\theta$ for the anti-quarks).

As an example we discuss the function $f_{A_0}(x_0, \theta)$ in some detail. It describes the creation of a (finite-volume) $\mathbf{p} = 0$ heavy-light pseudoscalar meson state, $|\varphi_B(L)\rangle$, through quark and antiquark boundary fields which are separately projected onto momenta $\mathbf{p} = \pm\mathbf{p}_\theta$. This state “propagates” an interval x_0 in Euclidean time. From the upper boundary a state with vacuum quantum numbers propagates a time-distance $T - x_0$. The correlation function $f_{A_0}(T/2, \theta)$ can thus be written in terms

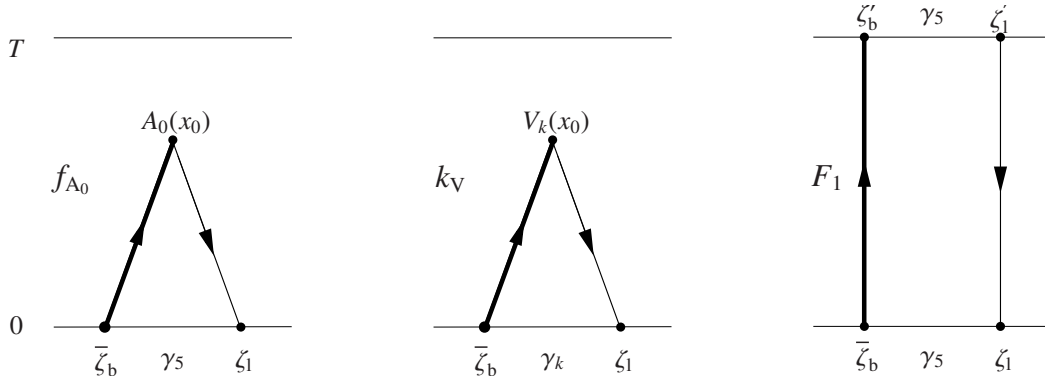


Figure 4: The Schrödinger functional correlation functions f_A , k_V and f_1 . For K_1 , in the rightmost diagram γ_5 is replaced by γ_k .

of Hilbert space matrix elements,

$$f_{A_0}(T/2, \theta) = \mathcal{Z}^{-1} \langle \Omega(L) | A_0 | B(L) \rangle, \quad (98)$$

$$|B(L)\rangle = e^{-T\mathbb{H}/2} |\varphi_B(L)\rangle, \quad (99)$$

$$|\Omega(L)\rangle = e^{-T\mathbb{H}/2} |\varphi_0(L)\rangle. \quad (100)$$

where \mathbb{H} is the QCD Hamiltonian and

$$\mathcal{Z} = \langle \Omega(L) | \Omega(L) \rangle. \quad (101)$$

$|\varphi_0(L)\rangle$ denotes the Schrödinger functional intrinsic boundary state. It has the quantum numbers of the vacuum. All states appearing in our analysis are eigenstates of total spatial momentum with eigenvalue zero. Their dependence on θ has been suppressed. The time evolution operator $e^{-T\mathbb{H}/2}$ suppresses high-energy states exponentially. When expanded in terms of eigenstates of the Hamiltonian, $|\Omega(L)\rangle$ and $|B(L)\rangle$ are thus dominated by contributions with energies of at most $\Delta E = \mathcal{O}(1/L)$ above the ground state energy in the respective channel (recall that we take $T = \mathcal{O}(L)$).

This explains why, at large time separation $x_0 \gg 1/m_h$, HQET is expected to describe the large-mass behavior of the correlation function, also in the somewhat unfamiliar framework of the Schrödinger functional.¹⁰

Equations similar to the above hold for $k_{\bar{V}}$; one only needs to replace pseudoscalar states by vector ones. Finally, the boundary-to-boundary correlator is represented as

$$F_1 = \mathcal{Z}^{-1} \langle B(L) | B(L) \rangle. \quad (102)$$

Since the boundary quark fields $\zeta, \bar{\zeta}, \dots$ are multiplicatively renormalizable [28], this holds also for the states $|\varphi_0(L)\rangle$ and $|\varphi_B(L)\rangle$.

¹⁰ More generally, HQET applies to correlation functions at large Euclidean separations.

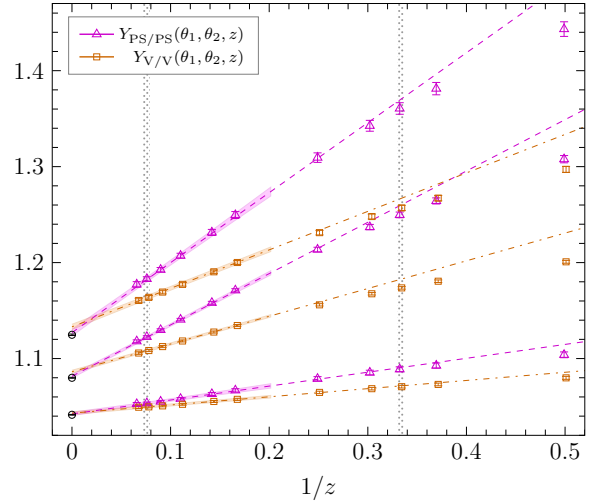


Figure 5: Extrapolations of $Y_{PS/PS}(\theta_1, \theta_2)$ and $Y_{V/V}(\theta_1, \theta_2)$ to the $M \rightarrow \infty$ limit for three combinations of (θ_1, θ_2) . The dimensionless heavy quark mass $z = ML$ is used as a variable. Black circles show the continuum results of the corresponding quantity computed in the static approximation. All data points were first extrapolated to the continuum limit [70]. Three different combinations of θ_1, θ_2 are shown, where $0 \leq \theta_i \leq 1$. Graph provided by P. Fritzsch, based on [70].

It now follows that the ratios

$$Y_{PS}(\theta) \equiv Z_A \frac{f_{A_0}(T/2, \theta)}{\sqrt{F_1(\theta)}}, \quad (103)$$

$$Y_V(\theta) \equiv -Z_V \frac{k_{\bar{V}}(T/2, \theta)}{\sqrt{K_1(\theta)}}, \quad (104)$$

$$Y_{PS/PS}(\theta_1, \theta_2) \equiv \frac{Y_{PS}(\theta_1)}{Y_{PS}(\theta_2)}, \quad (105)$$

$$Y_{V/V}(\theta_1, \theta_2) \equiv \frac{Y_V(\theta_1)}{Y_V(\theta_2)}, \quad (106)$$

are finite quantities. As is immediately clear from the

foregoing discussion,

$$Y_{\text{PS}}(L, M) = \frac{\langle \Omega(L) | \hat{A}_0 | B(L) \rangle}{\| |\Omega(L)\rangle \| \| |B(L)\rangle \|} \quad (107)$$

(or $Y_{\text{V}}(L, M)$) becomes proportional to the pseudoscalar (or vector) heavy-light decay constant as $L \rightarrow \infty$. At any fixed L , the large- M behavior of these quantities is indeed described by HQET if it is the correct effective theory.

Numerical tests of this equivalence were originally done in the quenched approximation [69], with $L \approx 0.2$ fm, profiting from the full improvement of the theory with mass-dependent improvement terms [71]. Here we show more recent results with $N_f = 2$ dynamical fermions. Based on the simulations [49] the following results are due to Fritzsche, Garron and Heitger [70].

The first two HQET predictions are

$$Y_{\text{PS/PS}}(\theta_1, \theta_2) = Y_{\text{stat}}(\theta_1, \theta_2) + \mathcal{O}(1/M) \quad (108)$$

$$Y_{\text{V/V}}(\theta_1, \theta_2) = Y_{\text{stat}}(\theta_1, \theta_2) + \mathcal{O}(1/M). \quad (109)$$

Due to spin symmetry, the static limit $Y_{\text{stat}}(\theta_1, \theta_2)$ is the same for the vector channel and the pseudoscalar channel. It can be computed by replacing the relativistic fields by the static ones. The comparison is shown in figure 5, extrapolating the relativistic results with just a linear function in $1/z$ for $z \equiv ML \geq 5$. Results of the extrapolation are in very good agreement with the numbers obtained directly in the static approximation, demonstrating at the same time the correctness of the effective theory and the usefulness of such observables for matching HQET to QCD.

Two more predictions read

$$\frac{Y_{\text{PS}}(\theta)}{C_{\text{PS}}(M/\Lambda)} = X_{\text{stat}}^{\text{RGI}}(\theta) + \mathcal{O}(1/M), \quad (110)$$

$$\frac{Y_{\text{V}}(\theta)}{C_{\text{V}}(M/\Lambda)} = X_{\text{stat}}^{\text{RGI}}(\theta) + \mathcal{O}(1/M).$$

The matrix element $X_{\text{stat}}^{\text{RGI}}$ is defined as Y_{PS} , but with the static quark field and it is the renormalization group invariant one, see eq. (57). For the time-component of the axial current, the factor $\varphi_{\text{stat}}(\bar{g})$ in that equation and the renormalisation factor $Z_{\text{A}}^{\text{stat, SF}}$ were determined non-perturbatively in a Schrödinger functional renormalization scheme [72]. Thus $X_{\text{stat}}^{\text{RGI}}$ is known without perturbative uncertainties.

The comparison is shown in figure 6. The agreement between the extrapolation of relativistic results and the static effective theory is not as convincing as in figure 5. In fact, for Y_{PS} there is a disagreement, but only at the level of 1-2 sigma. This may therefore be a statistical

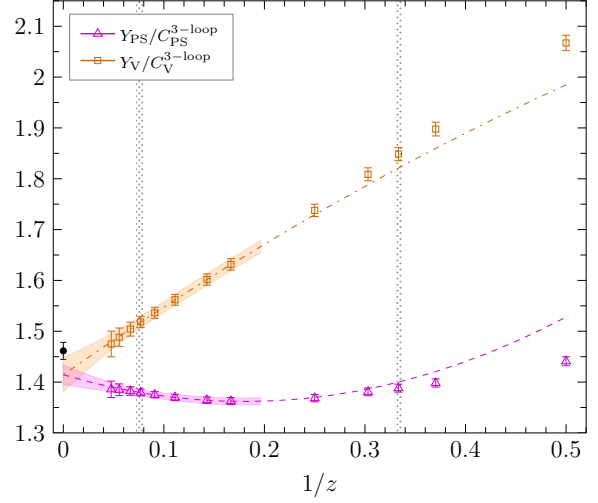


Figure 6: Comparison of static extrapolations of $Y_{\text{PS}}(\theta)$ and $Y_{\text{V}}(\theta)$ to the non-perturbative HQET results in the continuum (filled circle). Conversion functions $C_{\text{PS}}, C_{\text{V}}$ evaluated at 3-loop order of perturbation theory are used. The extrapolation, quadratic in $1/z$, uses data with $1/z < 0.2$ only. Graph provided by P. Fritzsche, based on [70].

effect, but it may also be due to the perturbative approximation of C_{PS} , which is somewhat doubtful as discussed earlier. In comparison, in figure 5 the perturbative factors $C_{\text{PS}}, C_{\text{V}}$ drop out.

We have only shown two out of a number of tests. Considering them all [69, 70], we conclude that the effective theory is very well tested, but it is safer not to use conversion functions $C_{\text{PS}}, C_{\text{V}}$ from perturbation theory, even if they are determined at three-loops, i.e. with relative errors of order $\bar{g}^6(m_*)$.

5. Numerical Simulations and results

We now turn to a discussion of numerical results skipping most of the details of the Monte Carlo simulations. These separate into two categories. One part concerns small volume simulations $L \leq 1$ fm with Schrödinger functional boundary conditions. These have been discussed in [73, 74, 75, 76, 77]. Many such simulations had to be carried out in order to control the renormalization and matching. They required tuning of the bare parameters such that continuum limits can be taken at a fixed volume in physical units and at vanishing dynamical quark mass.

A second part is then necessary in large volume, with $L \geq 2$ fm, $m_\pi L \geq 4$. These simulations are rather universally useful and also much more expensive in the numerical effort. Hence they have been carried out in coordination with several European groups, by the CLS

effort [78], see in particular [79]. The simulations were carried out down to pion masses of 200 MeV on lattices with up to 128×64^3 points. They were possible due to a significant improvement of algorithms and their implementations [80, 81, 82, 83, 84, 85, 86] starting from the principle of the HMC algorithm [87, 88]. For recent reviews covering lattice QCD algorithms we refer to [89, 90]. Some more details can be found in [91].

All HQET computations and strategies were developed and tested in the quenched approximation, i.e. QCD with all valence quarks but a vanishing number of sea quark flavors: $N_f = 0$. We will mention these results only for comparison, while we discuss the results with $N_f = 2$ quark flavors in more detail. A dynamical strange quark has not yet been included in the HQET simulations of the ALPHA collaboration.

5.1. The $B^* B \pi$ coupling.

As explained above, the available large volume simulations still have unphysical quark masses and results need to be extrapolated to the point where the light quark masses are the physical ones. The natural way to carry out such an extrapolation is with the help of a systematic expansion in the light quark mass. Again this means that one uses predictions from an effective field theory which implements the expansion. It is heavy meson chiral perturbation theory (HMChPT). The fields in this effective theory are a triplet of pion fields as well as a (static) B-meson and a B^* meson field. The expansion is a combined expansion in $1/m_h$, in the squared pion momenta and in the light quark mass, each counting as one power of the expansion variable, $\Lambda_{\text{QCD}}/m_h = O(\mathbf{p}^2/\Lambda_{\text{QCD}}^2) = O(m_{\text{up}}/\Lambda_{\text{QCD}})$, where as before we work in the B-meson rest frame.¹¹ At lowest order, the effective theory contains five parameters, usually called low energy constants. They all refer to the chiral limit and $m_h \rightarrow \infty$. There are the pion decay constant, f , the light-quark condensate, the mass of the B-meson and the three-point coupling $B^* B \pi$ denoted by \hat{g} [96, 97, 98]. Apart from \hat{g} the couplings can be taken from experiment (the light quark condensate is removed from the list by taking m_π^2 instead of m_{up} as mass-parameter). Typical predictions of HMChPT are

(with $\xi = m_\pi^2/(8\pi^2 f_\pi^2)$)

$$m_B = m_B^{\text{chir}} + f_\pi \left(3\sqrt{2}\pi^2 \hat{g}^2 \xi^{3/2} + \alpha_m \xi + O(\xi^2) \right) \quad (111)$$

and

$$\sqrt{\frac{m_B}{2}} f_B = \sqrt{\frac{m_B}{2}} f_B \Big|_{\text{chir}} \times \left[1 - \frac{3}{4} \frac{1 + 3\hat{g}^2}{2} \xi \log(\xi) + \alpha_f \xi + O(\xi^2) \right]. \quad (112)$$

The coefficients of the leading non-analytic terms, $\xi^{3/2}$ and $\xi \log(\xi)$, in eq. (111) and in eq. (112), respectively, are given in terms of \hat{g} . This coupling is therefore better determined before using the HMChPT formulae to extrapolate from unphysical quark masses to the physical one.

A determination of \hat{g} just means that HMChPT is matched to HQET at the lowest order in $1/m_h$; at this level HQET is regarded as the fundamental theory. The matching condition can be written to directly give \hat{g} via

$$\hat{g} = \frac{1}{2} \langle B^0(\mathbf{0}) | A_k^{\text{du}}(0) | B_k^{*+}(\mathbf{0}) \rangle, \quad (113)$$

$$A_\mu^{\text{du}}(x) = \bar{\psi}_d(x) \gamma_\mu \gamma_5 \psi_u(x), \quad (114)$$

where $\psi_d(\psi_u)$ annihilates a down(up) quark and the index $k = 1, 2, 3$ is not summed over. The non-relativistic normalization of states given earlier is used; in finite volume it is $\langle B^0(\mathbf{p}) | B^0(\mathbf{p}) \rangle = \langle B_k^*(\mathbf{p}) | B_k^*(\mathbf{p}) \rangle = 2L^3 = 2V$, where L is the linear size of the torus.

Profiting from a newly developed method for its computation [68], the matrix element eq. (114), was determined in [92] with a much better precision than it was possible before. A comparison to other computations is shown in figure 7 for various pion masses (i.e. dynamical quark masses) and lattice spacings.

The low energy constant \hat{g} is defined in the chiral limit. Therefore, the computations shown in figure 7 are extrapolated to $m_\pi^2 = 0$. The final uncertainties are dominated by the systematic uncertainty in this step. Ref. [92] obtained

$$\hat{g} = 0.492(29). \quad (115)$$

in the chiral limit.

5.2. HQET parameters

For $N_f = 0$ the HQET parameters ω_i have been determined in [99]. Here we review the refined strategy applied with two flavors of dynamical fermions [49]. It covered the three parameters in the action and the two parameters of A_0^{HQET} needed for the computation of f_B .

¹¹Usually, the second term is written as $O(\mathbf{p}^2/(8\pi^2 f_\pi^2))$ and the expansion coefficients are assumed to be order one in that variable. With a pion decay constant of $f \sim \Lambda_{\text{QCD}}/4$ for our previous estimate of $\Lambda_{\text{QCD}} \sim 500$ MeV, there is a numerical difference. Similar ambiguities are present in a prefactor of $m_{\text{up}}/\Lambda_{\text{QCD}}$, but these numerical factors do not influence the structure of the expansion and are not well known/defined anyway.

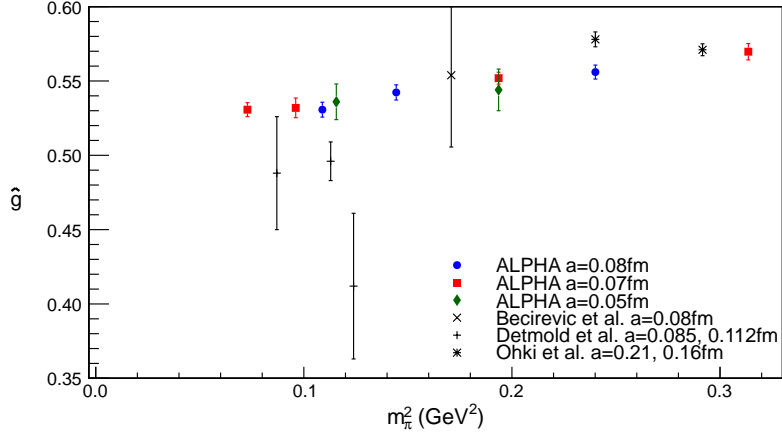


Figure 7: A summary of unquenched lattice QCD results for \hat{g} . The results from the three lattice spacings used in [92] are labeled ‘ALPHA’. Additionally there are results of Ohki et al. [93], Becirevic et al. [94] and Detmold et al. [95]. For Ref. [95], which employs $N_f = 2 + 1$ dynamical flavors, we take the results for a single level of link smearing in the static action. Graph from [92].

i	Φ_i^{QCD}	c.f.	large volume limit	dominant sensitivity to
1	$-L \frac{d}{dx_0} f_{A_0} \Big _{x_0=T/2}$	eq. (93)	Lm_B	m_{bare}
2	$\log(Y_{\text{PS}})$	eq. (105)	$\log(L^{3/2} f_B \sqrt{m_B})$	$\ln Z_{A_0}^{\text{HQET}}$
3	$\log(f_{A_0}(T/2, \theta_1)/f_{A_0}(T/2, \theta_2))$	eq. (105)	0	$c_{A_{0,1}}$
4	$\frac{1}{4} \log \left[\frac{F_1(\theta_1) K_1(\theta_1)^3}{F_1(\theta_2) K_1(\theta_2)^3} \right]_{T=L/2}$	eq. (95),(96)	0	ω_{kin}
5	$\frac{3}{4} \log[F_1/K_1]$	eq. (95),(96)	$L(m_{B^*} - m_B)$	ω_{spin}

Table 3: Matching observables and some of their properties.

All five used matching observables are similar to what we discussed in section 4. We list them in table 3. Note how three of them are small volume versions of physical quantities which one would like to predict in large volume. If finite volume effects are truly small, these quantities are then predicted correctly with very small truncation errors of the $1/m_h$ expansion. Even with significant finite volume effects, this property is expected to reduce truncation errors as compared to many other choices.

In static order, only Φ_1 , Φ_2 are needed and they are finite volume generalizations of mass and decay constant of the B-meson. In figure 8 we illustrate their determination. The observables are computed for various fixed $z = ML_1$ and fixed L_1 , but different resolutions $L_1/a = 20 \dots 40$. They are then extrapolated to the continuum limit using the asymptotic dominance of $(a/L_1)^2$ corrections. In order to carry this step out, one needs to

control the non-perturbative determination of the RGI mass M and one needs to know what fixed L means in terms of the bare parameters. Indeed, fixed L is only defined up to discretisation errors. Here it was chosen to mean fixed $\bar{g}_{\text{SF}}(L)$, the running coupling in the Schrödinger functional renormalization scheme. The required full control over the renormalization of QCD in the light sector had been gained in a series of earlier works. Some milestones are [73, 100, 77, 76, 101, 102], reviewed in some detail in [91].

The middle column of figure 8 shows the mass-dependence of Φ_i for $L = L_1$ where we match. The expected $\Phi_1 = O(M) = O(z)$ and $\Phi_2 = O(1)$ is clearly visible, also the $O(1/M) = O(1/z)$ corrections are seen in Φ_2 . The right column finally demonstrates the good control over the continuum limit in the scaling step to L_2 , eq. (81). It is only in this last step where the restriction to the static approximation is relevant at all. Still,

the graph does not look much different when the full system with five Φ_i is treated including the NLO corrections [49].

Let us now illustrate these NLO corrections. Figure 9 shows the other three observables after subtracting their static part. They clearly exhibit the $O(1/M) = O(1/z)$ behavior at large mass. Again this represents a confirmation of the correctness of HQET.

With these steps carried out, it is only left to evaluate eq. (82) at the desired lattice spacings where large volume simulations are carried out. The HQET parameters are then known as a function of the RGI mass M , more precisely $z = ML_1$ and at a few values of the lattice spacing corresponding to integer L_2/a . By an interpolation the knowledge of the parameters is extended to all values of the lattice spacing within the range corresponding to the accessible L_2/a . The correct value M_b for a b-quark in Nature still needs to be determined by matching the meson mass as a function of M to the experimental B-meson mass. This step yields also the first prediction of the theory, namely the physical value of the renormalized b-quark mass, which is one of the fundamental parameters of QCD. We turn to it now.

5.3. Mass of the b-quark

5.3.1. Static order

Lattice HQET computations of the b-quark mass have been carried out originally with a just perturbative subtraction of the $1/a$ divergence [106, 107, 108] in the static approximation. A continuum limit does not exist in this case, so a corresponding extrapolation may not be performed. Instead one can check for stability under changes of a . When present, such a stability indicates that divergent terms as well as discretisation effects are small. For comparison we include a world average of the year 2001 by S. Ryan [103] in our summary, table 4.

The first computations with non-perturbative renormalization were still restricted to the quenched approximation.: The initial static order result of [30] was later extended to a full NLO mass computation in [104].

5.3.2. HQET at NLO

Fairly recently a NLO HQET computation with $N_f = 2$ flavors of dynamical fermions based on the parameter determination discussed in the previous section was completed [105]. It used the GEVP method [67] for better control of the computation of the B-meson mass (at a fixed lattice spacing and other bare parameters such as m_h^{bare}) and exploited several CLS lattices. They cover three lattice spacings between $a = 0.048\text{fm}$ and $a = 0.075\text{fm}$ and several light-quark masses corresponding

to pion masses $190\text{ MeV} \leq m_\pi \leq 440\text{ MeV}$. At a fixed mass of the b-quark, parameterized by $z = ML$, these results needed to be extrapolated to the physical pion mass and to the continuum limit (all volumes are large enough to safely neglect finite volume corrections). This extrapolation was performed in the form of one global fit:

- The non-analytic term in the m_π^2 expansion, eq. (111), discussed in and known from section 5.1 is subtracted from the data.
- The remaining mass-dependence is parameterized by a linear term in m_π^2 ($\propto \xi$).
- The lattice spacing dependence is parameterized by the leading term in the Symanzik expansion, $\propto a^2$.
- The extrapolation is carried out simultaneously for two discretizations of HQET (HYP1/2). All fit-parameters except for the coefficient of a^2 are common to both discretizations.
- Physical units are taken from a previous extrapolation of the kaon decay constant to the physical point and continuum limit [79].

This parameterization of lattice spacing and quark mass dependence neglects higher order terms in a^2 and ξ , also the mixed term $a^2 \times \xi$. It fits the data very well. Data and fit, together with the continuum limit, are shown in figure 10 for three prescribed values of z .

The results at $a = 0$ and the physical pion mass were then interpolated in z and finally $z_b = M_b L_1$ was determined by requiring

$$m_B(z_b) = m_B^{\text{experimental}}. \quad (116)$$

for the interpolation function $m_B(z)$, see the right graph in figure 10. The resulting number $M_b = 6.58(17)\text{GeV}$ is included in our summary, table 4. Repeating the analysis with all $1/m_h$ terms dropped yields the static result. It is almost identical indicating that NNLO terms are very small. Note that a naive estimate of these terms, $\Lambda^3/m_b^2 \approx 4\text{MeV}$, is indeed very small compared to the dominating statistical errors.

The RGI mass M_b can be changed easily to m_* defined earlier, using a knowledge of the Λ -parameter [79] and inserting the $\overline{\text{MS}}$ 4-loop τ and β functions [37, 38, 39, 40] into eq. (57) and eq. (63).

These numbers (last row of table 4) are well controlled. Given the small difference to $N_f = 0$ results, it is even very hard to imagine that the missing strange quark is a significant source of error. The numbers agree with other determinations and the PDG average [109] of

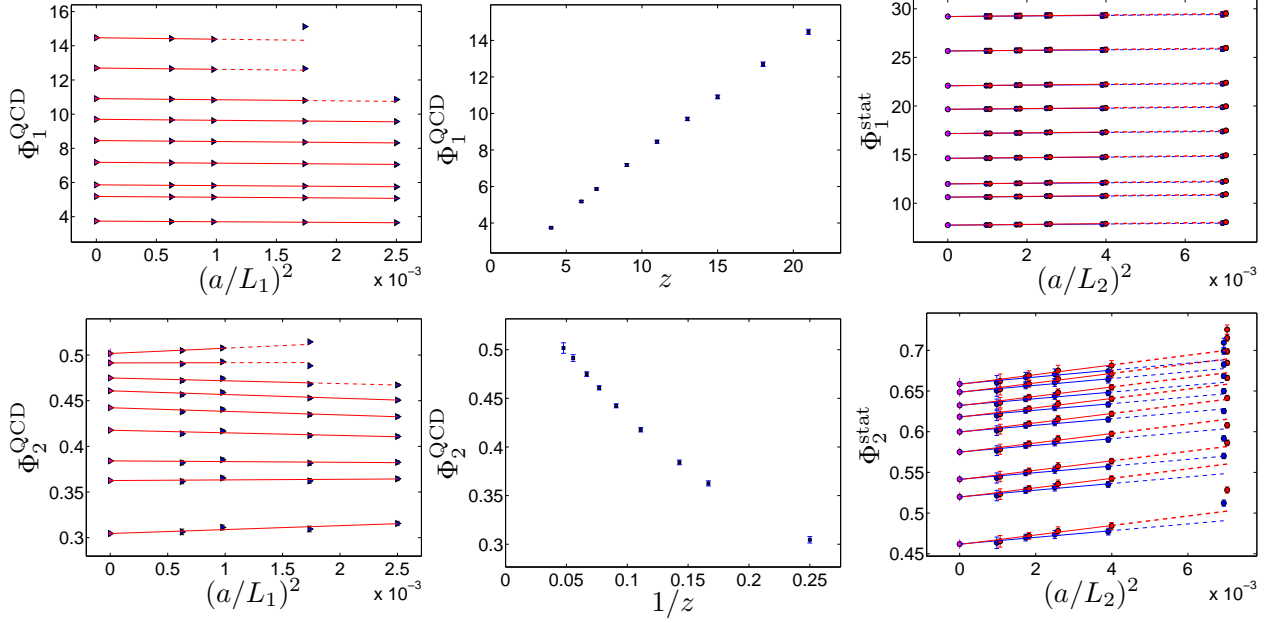


Figure 8: Continuum extrapolation of Φ_1 and Φ_2 in $L = L_1$ (left). Their resulting mass-dependence ($z = ML$, middle). On the right we show the step scaling to obtain them in $L = L_2$ in LO HQET. The b-quark in Nature has about $1/z \approx 0.08$.

N_f	ref.	remarks	$m_b(m_b)[\text{GeV}], \overline{\text{MS}}$		$M_b[\text{GeV}]$	
			static	$\mathcal{O}(1/m_h)$	static	$\mathcal{O}(1/m_h)$
0-2	[103]	2-loop subtracted; 2001 average	4.30(10)			
0	[30]	NP	4.12(7)(4)			
0	[104]	NP	4.32(5)	4.35(5)	6.81(8)	6.76(9)
2	[105]	NP	4.21(11)	4.21(11)	6.57(17)	6.58(17)

Table 4: HQET results for the RGI b-quark mass M_b and $m_* = m_b(m_b)$ in the $\overline{\text{MS}}$ scheme computed using lattice HQET. Results with perturbative subtraction of $1/a$ divergences are labeled “n-loop subtracted”. When renormalization and matching is treated non-perturbatively, we just have a label “NP”.

$m_{b*} = 4.18(3)$. They thus boost our confidence in having systematic errors in the determination of m_b under control.

5.4. B-meson decay constants

5.4.1. Mass-dependence

Before discussing the most up-to-date $N_f = 2$ results for the decay constants, we spend some time on an important theoretical aspect: what is the dependence of the decay constants on the heavy quark mass? Does the asymptotic mass-scaling eq. (71) even reach down to $m_h = m_c$ and how far is the b-quark from the heavy

quark limit? With good statistical and systematic precision, these questions have only been studied in the quenched approximation [104, 110]. For qualitative earlier results we refer to [112, 103]. In [110] the static matrix elements were first determined at three different lattice spacings increasing the precision by a use of translation invariance as well as the GEVP method. They were then extrapolated to the continuum limit as shown in figure 11. Only the B_s meson was investigated because the chiral limit is singular in the quenched approximation, rendering computations of the limit of very light quarks rather meaningless.

The static result for the ground state is compared to

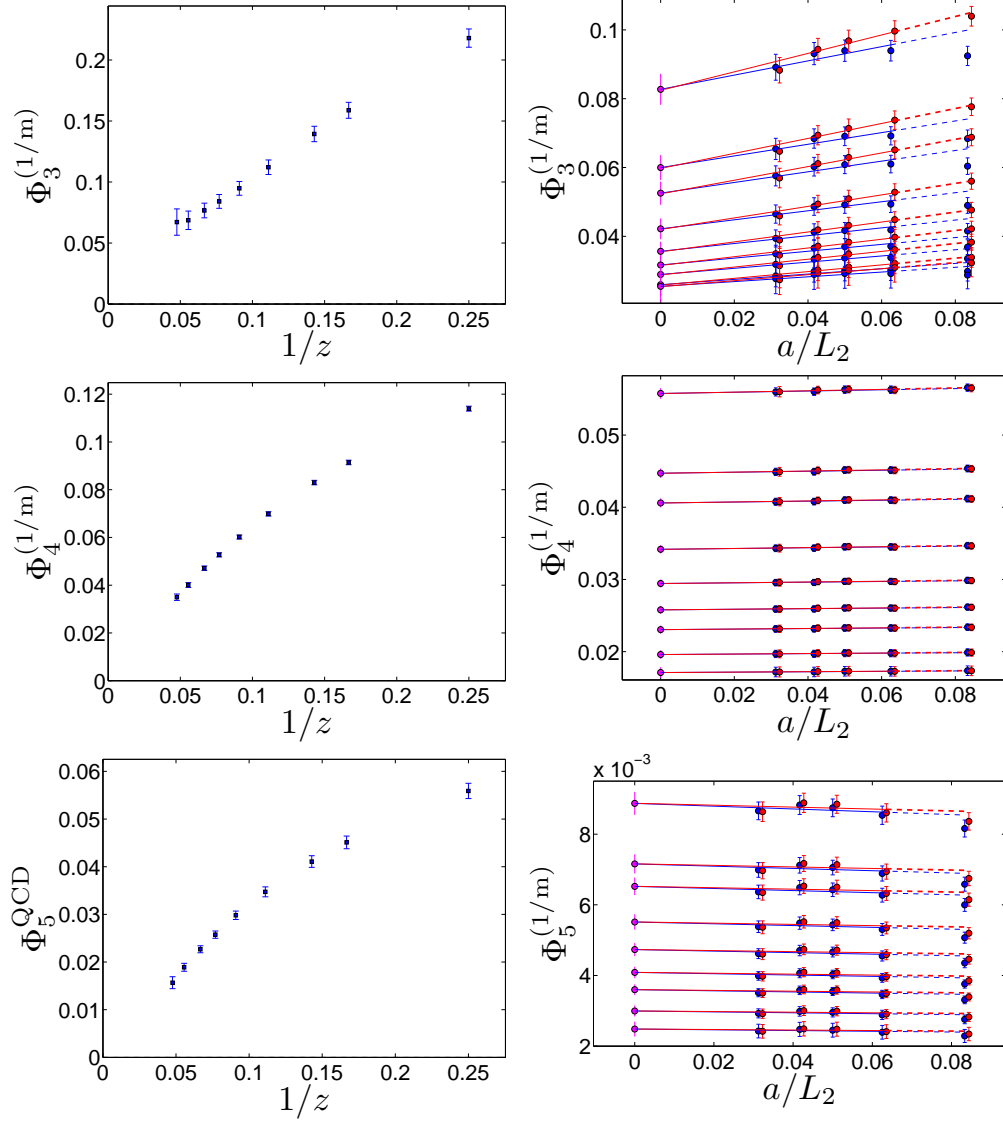


Figure 9: $\Phi_i^{(1/m_h)}(L_1) = \Phi_i^{QCD}(L_1) - \eta_i(L_1)$, $i = 3, 4$ in L_1 on the left and their step scaling function to obtain $\Phi_i^{(1/m_h)}(L_2) = \Phi_i^{QCD}(L_2) - \eta_i(L_2)$ on the right. The bottom line shows $\Phi_5(L_1)$; spin symmetry means that its static part vanishes, $\eta_5 = 0$. The b-quark in Nature has about $1/z \approx 0.08$.

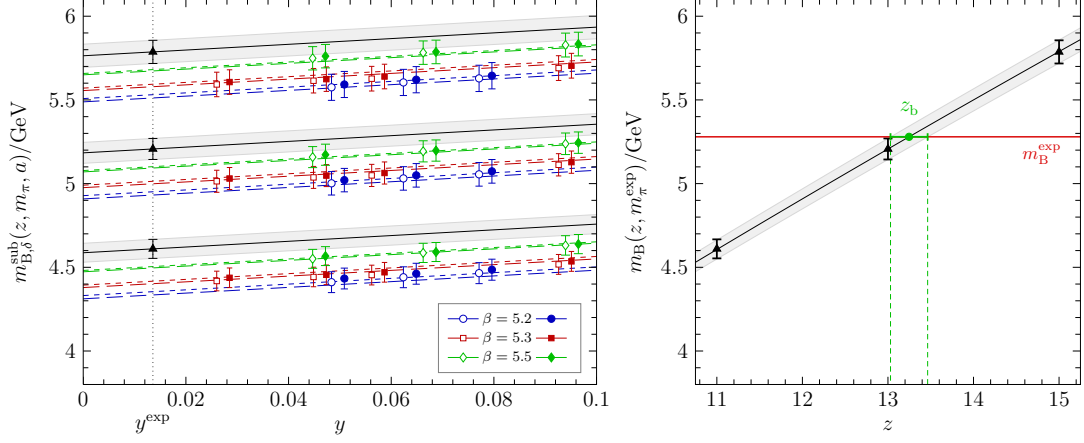


Figure 10: Left: Chiral and continuum extrapolation of m_B for the z -values used in the determination of z_b . Open/filled symbols refer to HYP1/HYP2 data points as do long/short dashed curves, respectively. The continuum pion mass dependence is given by the solid lines together with a shaded error band. The triangle shows the estimated continuum limit at the physical pion mass. The figure uses a notation $y = \xi$ and δ is an index for the different discretizations.

Right: Interpolation to z_b by imposing eq. (116). Graphs from [105].

N_f	ref.	remarks	$f_B[\text{MeV}]$		$f_{B_s}[\text{MeV}]$		f_{B_s}/f_B	
			static	$O(1/m_h)$	static	$O(1/m_h)$	static	$O(1/m_h)$
0	[112]	summary PT	276(55)(19)				1.22(4)(2)	
0	[110]	NP			229(3)	216(5)		
2	[113]	NP	190(5)(2)	186(13)	226(6)(9)	224(14)	1.189(24)(30)	1.203(65)
2+1	[114]	PT, 1-loop	219(17)		264(19)		1.193(41)	
2	[115]	FLAG average ¹	189(8)		228(8)		1.206(24)	
2+1	[115]	FLAG average ¹	190.5(4.2)		227.7(4.5)		1.202(22)	

Table 5: Results for the B-meson decay constant computed using lattice HQET in the upper part. Results with with completely perturbative renormalization are labeled by “PT”. When renormalization and matching is treated non-perturbatively, we just label “NP”.

¹ The FLAG averages in the lower part combine various methods, not just HQET.

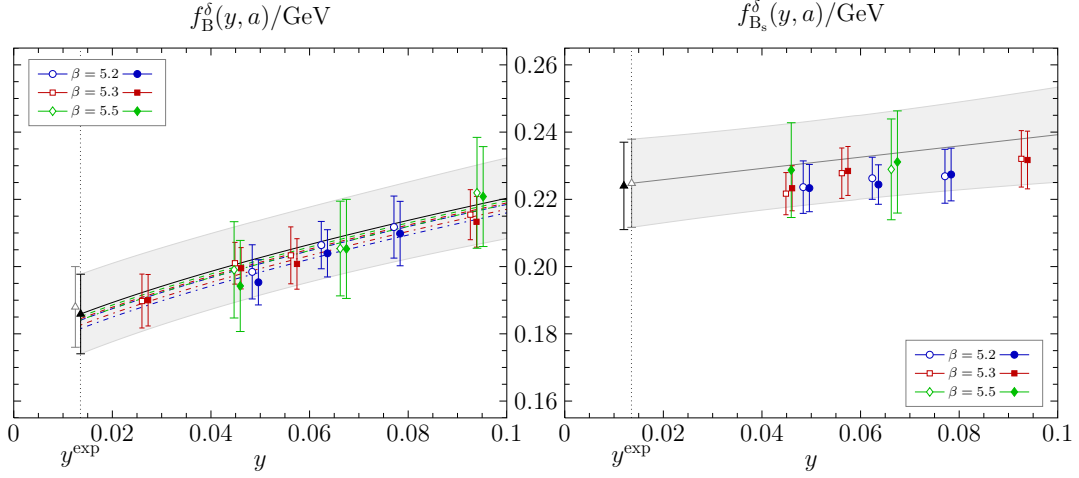


Figure 13: Extrapolation of the B (left panel) and B_s (right panel) meson decay constant to the physical point. On the left, the extrapolation using $\text{HM}\chi\text{PT}$ at NLO (filled triangle) is compared to a linear one (open triangle), in order to extract the systematic error from truncating $\text{HM}\chi\text{PT}$ at NLO. For f_{B_s} only a LO formula is known and shown. As a comparison also the final result, the continuum value of $f_{B_s} = [f_{B_s}/f_B]f_B$ is shown. Figure from [113].

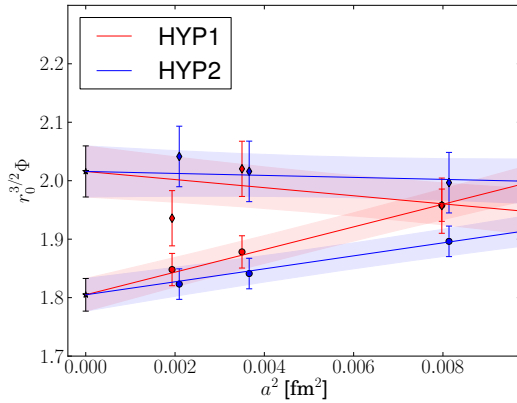


Figure 11: Continuum limit of the $N_f = 0$ static matrix element $\Phi = \langle 0 | A_0^{\text{stat}} | B \rangle$ in RGI normalization. The lower part shows the ground state matrix element and the upper part the first excited state with the quantum number of the B-meson. Graph from [110]

results at finite mass in figure 12. The graph shows $f_{\text{PS}} \sqrt{m_{\text{PS}}}/C_{\text{PS}}$, where PS is a strange-heavy pseudo-scalar against the inverse heavy meson mass. At the lowest order, the meson mass is proportional to the quark mass. Therefore m_{PS} can be taken as a proxy for the quark mass. The conversion function C_{PS} is computed with the full perturbative knowledge, i.e. it has relative errors of order $\alpha(m_h)^4$. However, as discussed before, for b- or c- quark masses it is not at all clear that the perturbative errors are negligible.

The graph shows a very consistent picture, with the

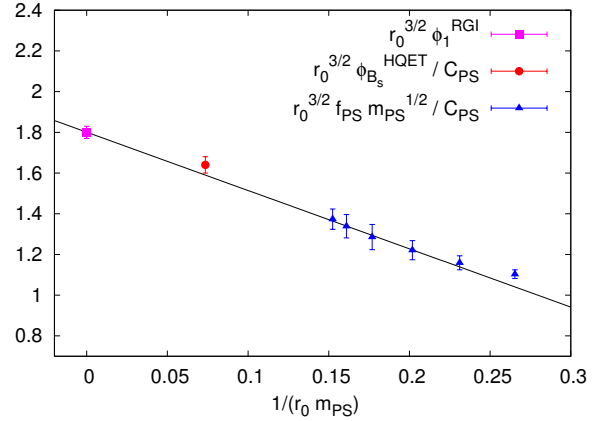


Figure 12: $N_f = 0$ heavy quark mass dependence of the heavy-strange decay constant. All dimension-full quantities are expressed in units of $r_0 \approx 0.5\text{fm}$ [111]. The charm quark is located at about $m_{\text{PS}} r_0 = 0.2$ and the b-quark at $m_{\text{PS}} r_0 = 0.07$. Graph from [110].

static limit computation on the left being in line with the relativistic data points on the right *and* an HQET computation with non-perturbative matching and including the $1/m_h$ terms at $m_{\text{PS}} = m_B$. Given the somewhat uncertain status of the perturbative C_{PS} , the good agreement with a simple linear behavior in $1/m_{\text{PS}} \sim 1/m_h$ over a large range is in fact somewhat surprising.

In the above discussion of the mass-dependence it is hard to get around a perturbatively extracted C_{PS} .¹²

¹²Non-perturbative definitions of C_{PS} do not separate the logarithm-

Without it taking care of the logarithmic modifications of the naive scaling law the curve in figure 12 would not even have a finite limit at $1/m_h = 0$. However, for predictions at the b-quark mass (or any other large mass), the non-perturbative HQET parameters ω_i from section 5.2 can be used. From now on we only discuss ALPHA collaboration results obtained in this entirely non-perturbative way. Only in the comparison to results in the literature perturbatively renormalized results by other groups are shown.

5.4.2. HQET results with non-perturbative parameters

The physical value of the b-quark mass (parameterized by z_b) is known from the previous section. All HQET parameters are then interpolated to that quark mass. Once they are known, the computation of the decay constants is in principle straight forward. However, again care has to be taken about several limits.

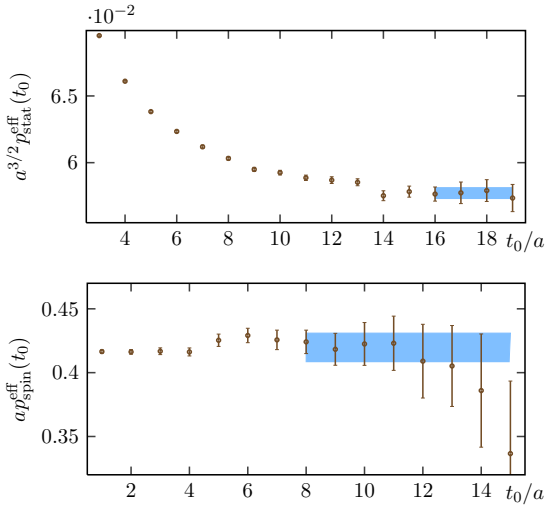


Figure 14: Plateau averages after applying the GEVP analysis to data obtained on the $N_f = 2$ CLS ensemble N6 ($a = 0.048$ fm, $m_\pi = 340$ MeV). The upper plot shows the B_s -meson static matrix element p_{stat} . The lower plot shows the chromo-magnetic matrix element p_{spin} . Note eq. (117) for how these terms enter in the expression for the decay constant. Figure from [113].

1) for each lattice spacing, volume and light quark mass, the decay constant has to be extracted from the large-time limit of correlation functions. One usually forms ratios of correlation functions which have the decay constant as their large time ($=t$) limit and asymptotic corrections to it of order¹³ $\Delta E_{2,1} t \exp(-\Delta E_{2,1} t)$.

¹³mic corrections from power corrections.

¹³The pre-factor $\Delta E t$ is present since we are dealing with an effective theory computation, see [113].

Here, t is the time extent of the two-point functions entering and $\Delta E_{n,1} = E_n - E_1$ is the difference of the indicated energy levels; $\Delta E_{2,1}$ is around 600 MeV. Alternatively, with the GEVP method, the dominant corrections can be changed to $O(\Delta E_{n,1} t_0 \exp(-\Delta E_{n,1} t_0))$ with a larger n . At the same time, a second time separation t_0 is present in the GEVP which in practice is $t_0 = t/2$. For a proper explanation we have to refer to [67, 113]. The analysis in the latter reference estimates the correction term from the results at smaller t_0 and then uses t_0 large enough such that the estimated correction is a factor three below the statistical error of the final result. We show two such plateau analysis for the B_s meson in figure 14. The plotted quantities $p_{\text{stat}}, p_{\text{spin}}$ enter the decay constant through the HQET expansion

$$\begin{aligned} f_{B_s} &= \exp(\chi) / \sqrt{a^3 m_{B_s} / 2}, \\ \chi &= \ln(Z_{A_0}^{\text{HQET}}) + \ln(a^{3/2} p_{\text{stat}}) \\ &\quad + \omega_{\text{kin}} p_{\text{kin}} + \omega_{\text{spin}} p_{\text{spin}} + c_{A_0,1} p_{A_0^{(1)}}. \end{aligned} \quad (117)$$

The chosen start of the plateau averages according to the explained criterion look overly conservative in the plot, but on the other hand, excited state contaminations are clearly visible in the static piece, p_{stat} , and they are also hard to rule out for the $1/m_h$ term shown.

In summary, obtaining the ground state matrix element is far from trivial, but within the rather conservative errors of [113] it appears to be under control. We do not want to hide that the statistical errors for the B-meson (rather than B_s) are somewhat larger, see Figure 1 of [113].

2) A continuum extrapolation has to be carried out and

3) the results have to be extrapolated to the physical quark mass.

Just like in the case of the meson mass, 2) and 3) are carried out in one global fit. As seen in figure 13, the lattice spacing dependence is not significant at all and one could just average the numbers at the different lattice spacings. However, this would not account for the uncertainty in the statement that the a -dependence is insignificant. Therefore, as above, an a^2 term is fitted. The light-quark-mass dependence is parameterized as a linear dependence and alternatively as the one predicted by heavy meson chiral perturbation theory. The difference in the extrapolated value is very small and accounted for in the errors.

4) In principle we should also worry about effects of the finite volume, but these are very small for the considered volumes.

The resulting numbers are listed in table 5 together

with the previously computed $N_f = 0$ decay constants.¹⁴ The latter were quoted as [110]

$$r_0^{3/2} f_{B_s}^{\text{stat}} \sqrt{m_{B_s}} = 2.14(4), \quad (118)$$

$$r_0^{3/2} f_{B_s}^{\text{HQET}} \sqrt{m_{B_s}} = 2.02(5). \quad (119)$$

We combine them with the present estimate $r_0 = 0.50(2)$ fm (see [117]) to $f_{B_s}^{\text{stat}} = 229(3)(10)$ MeV and $f_{B_s}^{\text{HQET}} = 216(5)(9)$ MeV. In the table we also show older numbers as well as the recent computation by the RBC/UKQCD collaboration [118, 114]. All of these use a perturbative renormalization. The apparent difference between 2+1 and 2 flavor results in the static approximation are likely due to the different renormalization and matching. We remind the reader that static results have a dependence on the matching condition which is of order $1/m_h$. It would therefore be premature to conclude that the difference between the static numbers in the table is due to perturbative renormalization.

As a separate result, it was also observed, in the continuum limit of the $N_f = 0$ theory, that the decay constant of the excited state is larger than the ground state decay constant by the following amount [110]:

$$\frac{f_{B_s'}^{\text{stat}} \sqrt{m_{B_s'}}}{f_{B_s}^{\text{stat}} \sqrt{m_{B_s}}} = 1.24(7) \quad \text{for } N_f = 0. \quad (120)$$

A careful continuum limit was needed to observe this splitting of decay constants, see figure 11. Still it is in agreement with an older investigation where a -effects were not yet controlled [119].

6. Conclusions, opportunities and challenges

So far, numerical results of non-perturbative HQET have been obtained only in the theory with at most two dynamical quark flavors. The dominant impact of the project described here concerns the concept, the methodology and the qualitative features of the HQET expansion. It has been shown that this works out, in principle and in practice. Having said that, we would like to emphasize, however, that the numbers in table 4 and table 5 provide a very valuable crosscheck on other results for flavor physics, even if they are obtained with just up and down quarks as dynamical quarks. The reason is that there is overwhelming numerical evidence

¹⁴Earlier $N_f = 0$ static results are summarised in [112]. A later static decay constant at a single lattice spacing is found in [116]. The results of [110] are much more precise and do have a continuum limit extrapolation.

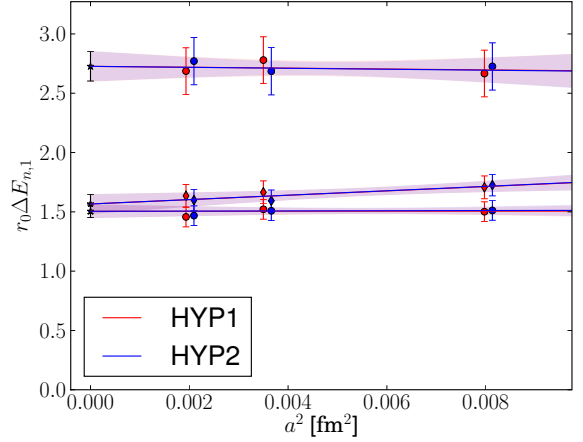


Figure 15: Continuum limits (stars) of $\Delta E_{n,1}^{\text{stat}}$ (circles) and $\Delta E_{n,1}^{\text{HQET}}$ (diamonds). Shown are the results for both HYP1 (red, shifted to the left) and HYP2 (blue, shifted to the right). Graph from [121].

that strange quark loop effects are strongly suppressed when one looks at the low energy properties of QCD [115, 120]. Therefore, it is very reasonable to expect present uncertainties to be dominated by the errors in renormalization and matching or in the assumptions made on the size of lattice spacing effects or the associated extrapolations. In these respects, HQET is on very solid theoretical grounds. There are no doubts about its renormalizability and the existence of the continuum limit, even if these properties are not proven to all orders of perturbation theory (see section 1.6). Renormalization and matching is carried out non-perturbatively without any compromise.

A crucial question concerning any expansion is of course how large truncation errors are. First of all, we do not expect the HQET expansion to be a convergent one. This does not matter, good asymptotic expansions are just fine, especially if one is able to compute only a few terms anyway. Looking at the size of the computed corrections, it is important to remember that they do depend on the matching conditions (see section 2.5). The way we (mostly) perform the matching, HQET is used to compute the finite size effects between e.g. a finite volume definition of a decay constant and the true large volume one. Apart from the fact that for B-physics we are expanding in a truly small parameter $\Lambda/m_b \approx 1/10$, this is one explanation for the very small NLO corrections that were found. However, there are cases where a priori we do not have a reason to expect such additional suppressions due to the matching condition. One such case is the splitting between ground state and first (“radially”) excited state of a B-meson [121]. Its con-

tinuum limit in the quenched approximation is shown in the lower part of figure 15. It is remarkable that there is no significant difference between the pure static result and the one including $1/m_h$ corrections after the continuum limit has been taken. In numbers, the static splitting is $r_0\Delta E_{2,1}^{\text{stat}} = 1.50(5)$ while $r_0\Delta E_{2,1}^{(1/m)} = 0.03(6)$ which is a bit smaller than expected from a simple $1.50 \times \Lambda/m_b \approx 0.15$ estimate.

There are good opportunities for improving the present numerical results in the near future. They arise because the uncertainties are (apart from the truncation error which we discussed is small) by far dominated by statistical errors apart from, maybe, the one coming from the omission of the strange quark vacuum polarization. The latter will be removed by the new set of large volume CLS simulations [122] (and the associated matching program) and there is also plenty of room to enhance the precision in the finite volume matching and step scaling.

There is also a very good opportunity to help in the understanding of the so-called V_{ub} puzzle, which says that this CKM matrix element differs between different determinations. Form factors of semi-leptonic B-decays are a key to understanding the puzzle. Work on them requires an extended program to match the full set of currents [51, 52, 53, 54] as well as the computation of form factors in large volume HQET [123, 124, 125]. We refer to [55] for a review.

Let us finish with a challenge for the future. It is the exponential deterioration of the signal-to-noise ratio, eq. (91). There are two issues. The first is that E_{stat} has a linear divergence which means the problem becomes worse as we approach the continuum limit further. As we have explained in section 3 this issue is not so severe since the coefficient of the $1/a$ divergence is very small for the HYP2 static action. However, the finite part is not small and leads to rather short plateaus, see figure 14. Formula (91) holds for our standard estimators of the correlation functions and the standard importance sampling. We should not give up to think about whether there are ways around it and see long plateaus with small errors in the future.

Acknowledgements

We would like to acknowledge our collaborators in this project, F. Bahr, F. Bernardoni, B. Blossier, J. Bulava, M. Della Morte, M. Donnellan, S. Dür, P. Fritzsche, N. Garron, A. Gérardin, D. Hesse, J. Heitger, G. von Hippel, A. Joseph, A. Jüttner, H. B. Meyer, M. Papinutto, A. Ramos, J. Rolf, S. Schaefer, A. Shindler and H. Simma as well as many many fruitful discussions with other

colleagues in the ALPHA Collaboration. We would further like to thank Martin Lüscher for advise, encouragement and for founding the ALPHA collaboration. We are grateful to Martin Beneke and Patrick Fritzsche for very useful comments on earlier versions of this text.

We are grateful for the support of the Deutsche Forschungsgemeinschaft (DFG) in the SFB/TR 09 “Computational Particle Physics” and we have profited from the scientific exchange in the SFB.

Lastly, the results described here are also due to a lot of support in the form of computational resources. We gratefully acknowledge the Gauss Centre for Supercomputing (GCS) for providing computing time through the John von Neumann Institute for Computing (NIC) on the GCS share of the supercomputer JUQUEEN at Jülich Supercomputing Centre (JSC). GCS is the alliance of the three national supercomputing centres HLRS (Universität Stuttgart), JSC (Forschungszentrum Jülich), and LRZ (Bayerische Akademie der Wissenschaften), funded by the German Federal Ministry of Education and Research (BMBF) and the German State Ministries for Research of Baden-Württemberg (MWK), Bayern (StMWFK) and Nordrhein-Westfalen (MIWF). We acknowledge PRACE for awarding us access to resource JUQUEEN in Germany at Jülich and to resource SuperMUC based in Germany at LRZ, Munich. We thank DESY for access to the PAX cluster in Zeuthen.

References

- [1] M. Neubert, Heavy quark symmetry, Phys. Rept. 245 (1994) 259–396. [arXiv:hep-ph/9306320](#).
- [2] A. V. Manohar, M. B. Wise, Heavy quark physics, Camb.Monogr.Part.Phys.Nucl.Phys.Cosmol. 10 (2000) 1–191.
- [3] A. Grozin, Heavy quark effective theory, Springer Tracts Mod.Phys. 201 (2004) 1–213. doi:10.1007/b79301.
- [4] R. Sommer, Non-perturbative QCD: Renormalization, O(a)-improvement and matching to heavy quark effective theory [arXiv:hep-lat/0611020](#).
- [5] R. Sommer, Introduction to Non-perturbative Heavy Quark Effective Theory. , in *Modern perspectives in lattice QCD*, editors: L. Lellouch, R. Sommer, B. Svetitsky, A. Vladikas and L. F. Cugliandolo, Oxford Univ. Pr., Oxford, UK [arXiv:1008.0710](#).
- [6] G. Colangelo, S. Durr, C. Haefeli, Finite volume effects for meson masses and decay constants, Nucl.Phys. B721 (2005) 136–174. [arXiv:hep-lat/0503014](#), doi:10.1016/j.nuclphysb.2005.05.015.
- [7] G. Colangelo, S. Durr, The Pion mass in finite volume, Eur.Phys.J. C33 (2004) 543–553. [arXiv:hep-lat/0311023](#), doi:10.1140/epjc/s2004-01593-y.
- [8] G. Colangelo, S. Durr, R. Sommer, Finite size effects on $M(\pi)$ in QCD from chiral perturbation theory, Nucl.Phys.Proc.Suppl. 119 (2003) 254–256. [arXiv:hep-lat/0209110](#), doi:10.1016/S0920-5632(03)80450-4.

- [9] K. Symanzik, Continuum Limit and Improved Action in Lattice Theories. 1. Principles and ϕ^4 Theory, Nucl.Phys. B226 (1983) 187. doi:10.1016/0550-3213(83)90468-6.
- [10] K. Symanzik, Continuum Limit and Improved Action in Lattice Theories. 2. $O(N)$ Nonlinear Sigma Model in Perturbation Theory, Nucl.Phys. B226 (1983) 205. doi:10.1016/0550-3213(83)90469-8.
- [11] M. Lüscher, P. Weisz, On-Shell Improved Lattice Gauge Theories, Commun.Math.Phys. 97 (1985) 59. doi:10.1007/BF01206178.
- [12] C. McNeile, C. Davies, E. Follana, K. Hornbostel, G. Lepage, Heavy meson masses and decay constants from relativistic heavy quarks in full lattice QCD, Phys.Rev. D86 (2012) 074503. arXiv:1207.0994, doi:10.1103/PhysRevD.86.074503.
- [13] S. Weinberg, Phenomenological Lagrangians, Physica A96 (1979) 327.
- [14] M. Lüscher, S. Sint, R. Sommer, P. Weisz, Chiral symmetry and $O(a)$ improvement in lattice QCD, Nucl. Phys. B478 (1996) 365–400. arXiv:hep-lat/9605038.
- [15] C. Itzykson, J. B. Zuber, QUANTUM FIELD THEORY New York, Usa: Mcgraw-hill (1980) 705 P.(International Series In Pure and Applied Physics).
- [16] J. Korner, G. Thompson, The Heavy mass limit in field theory and the heavy quark effective theory, Phys.Lett. B264 (1991) 185–192. doi:10.1016/0370-2693(91)90725-6.
- [17] T. Mannel, W. Roberts, Z. Ryzak, A derivation of the heavy quark effective lagrangian from qcd, Nucl. Phys. B368 (1992) 204–220.
- [18] M. Della Morte, A. Shindler, R. Sommer, On lattice actions for static quarks, JHEP 0508 (2005) 051. arXiv:hep-lat/0506008, doi:10.1088/1126-6708/2005/08/051.
- [19] E. Eichten, B. R. Hill, An Effective Field Theory for the Calculation of Matrix Elements Involving Heavy Quarks, Phys.Lett. B234 (1990) 511. doi:10.1016/0370-2693(90)92049-0.
- [20] V. Dotsenko, S. Vergeles, Renormalizability of Phase Factors in the Nonabelian Gauge Theory, Nucl.Phys. B169 (1980) 527. doi:10.1016/0550-3213(80)90103-0.
- [21] J.-L. Gervais, A. Neveu, The Slope of the Leading Regge Trajectory in Quantum Chromodynamics, Nucl.Phys. B163 (1980) 189. doi:10.1016/0550-3213(80)90397-1.
- [22] I. Y. Arefeva, QUANTUM CONTOUR FIELD EQUATIONS, Phys.Lett. B93 (1980) 347–353. doi:10.1016/0370-2693(80)90529-8.
- [23] R. A. Brandt, F. Neri, M.-a. Sato, Renormalization of Loop Functions for All Loops, Phys.Rev. D24 (1981) 879. doi:10.1103/PhysRevD.24.879.
- [24] H. Dorn, Renormalization of Path Ordered Phase Factors and Related Hadron Operators in Gauge Field Theories, Fortsch.Phys. 34 (1986) 11–56. doi:10.1002/prop.19860340104.
- [25] A. Grozin, Heavy quark effective theory, Springer Tracts Mod.Phys. 201 (2004) 1–213. doi:10.1007/b79301.
- [26] M. Lüscher, R. Narayanan, P. Weisz, U. Wolff, The Schrodinger functional: A Renormalizable probe for non-Abelian gauge theories, Nucl.Phys. B384 (1992) 168–228. arXiv:hep-lat/9207009, doi:10.1016/0550-3213(92)90466-0.
- [27] S. Sint, On the Schrodinger functional in QCD, Nucl.Phys. B421 (1994) 135–158. arXiv:hep-lat/9312079, doi:10.1016/0550-3213(94)90228-3.
- [28] S. Sint, One loop renormalization of the QCD Schrodinger functional, Nucl.Phys. B451 (1995) 416–444. arXiv:hep-lat/9504005, doi:10.1016/0550-3213(95)00352-S.
- [29] M. Golterman, Applications of chiral perturbation theory to lattice QCD. , in *Modern perspectives in lattice QCD*, editors: L. Lellouch, R. Sommer, B. Svetitsky, A. Vladikas and L. F. Cugliandolo, Oxford Univ. Pr., Oxford, UK (2011) 423–515 arXiv:0912.4042.
- [30] J. Heitger, R. Sommer, Nonperturbative heavy quark effective theory, JHEP 0402 (2004) 022. arXiv:hep-lat/0310035, doi:10.1088/1126-6708/2004/02/022.
- [31] L. Maiani, G. Martinelli, Current Algebra and Quark Masses from a Monte Carlo Simulation with Wilson Fermions, Phys.Lett. B178 (1986) 265. doi:10.1016/0370-2693(86)91508-X.
- [32] M. Lüscher, S. Sint, R. Sommer, H. Wittig, Nonperturbative determination of the axial current normalization constant in $O(a)$ improved lattice QCD, Nucl. Phys. B491 (1997) 344–364. arXiv:hep-lat/9611015.
- [33] M. A. Shifman, M. B. Voloshin, On annihilation of mesons built from heavy and light quark and anti- $b_0 \rightarrow \bar{c} b_0$ oscillations, Sov. J. Nucl. Phys. 45 (1987) 292.
- [34] H. D. Politzer, M. B. Wise, Phys. Lett. B206 (1988) 681.
- [35] A. Borrelli, C. Pittori, Improved renormalization constants for b -decay and $b\bar{b}$ mixing, Nucl. Phys. B385 (1992) 502–524.
- [36] M. Kurth, R. Sommer, Heavy quark effective theory at one-loop order: An explicit example, Nucl. Phys. B623 (2002) 271–286. arXiv:hep-lat/0108018.
- [37] T. van Ritbergen, J. A. M. Vermaseren, S. A. Larin, The four loop beta function in quantum chromodynamics, Phys. Lett. B400 (1997) 379–384. arXiv:hep-ph/9701390.
- [38] K. G. Chetyrkin, Quark mass anomalous dimension to $O(\alpha_s^4)$, Phys. Lett. B404 (1997) 161–165. arXiv:hep-ph/9703278.
- [39] J. A. M. Vermaseren, S. A. Larin, T. van Ritbergen, The four loop quark mass anomalous dimension and the invariant quark mass, Phys. Lett. B405 (1997) 327–333. arXiv:hep-ph/9703284.
- [40] M. Czakon, The Four-loop QCD beta-function and anomalous dimensions, Nucl.Phys. B710 (2005) 485–498. arXiv:hep-ph/0411261, doi:10.1016/j.nuclphysb.2005.01.012.
- [41] D. J. Broadhurst, A. G. Grozin, Two-loop renormalization of the effective field theory of a static quark, Phys. Lett. B267 (1991) 105–110.
- [42] K. G. Chetyrkin, A. G. Grozin, Three-loop anomalous dimension of the heavy-light quark current in HQET, Nucl. Phys. B666 (2003) 289–302. arXiv:hep-ph/0303113.
- [43] X. Ji, M. J. Musolf, Subleading logarithmic mass dependence in heavy meson form-factors, Phys. Lett. B257 (1991) 409.
- [44] D. J. Broadhurst, A. G. Grozin, Matching qcd and HQET heavy-light currents at two loops and beyond, Phys. Rev. D52 (1995) 4082–4098. arXiv:hep-ph/9410240.
- [45] V. Gimenez, Two loop calculation of the anomalous dimension of the axial current with static heavy quarks, Nucl. Phys. B375 (1992) 582–624.
- [46] P. Weisz, Renormalization and lattice artifacts, in *Modern perspectives in lattice QCD*, editors: L. Lellouch, R. Sommer, B. Svetitsky, A. Vladikas and L. F. Cugliandolo, Oxford Univ. Pr., Oxford, UK .
- [47] S. Capitani, et al., Local bilinear operators on the lattice and their perturbative renormalization including $O(a)$ effects arXiv:hep-lat/9711007.
- [48] S. Bekavac, A. Grozin, P. Marquard, J. Piclum, D. Seidel, et al., Matching QCD and HQET heavy-light currents at three loops, Nucl.Phys. B833 (2010) 46–63. arXiv:0911.3356, doi:10.1016/j.nuclphysb.2010.02.025.
- [49] B. Blossier, M. Della Morte, P. Fritzsch, N. Garron, J. Heitger,

- R. Sommer, H. Simma, N. Tantalo, Parameters of Heavy Quark Effective Theory from $N_f = 2$ lattice QCD, JHEP 1209 (2012) 132. [arXiv:1203.6516](#), doi:10.1007/JHEP09(2012)132.
- [50] M. Lüscher, P. Weisz, U. Wolff, A Numerical method to compute the running coupling in asymptotically free theories, Nucl.Phys. B359 (1991) 221–243. doi:10.1016/0550-3213(91)90298-C.
- [51] M. Della Morte, S. Dooling, J. Heitger, D. Hesse, H. Simma, Matching of heavy-light flavor currents between HQET at order $1/m$ and QCD: I. Strategy and tree-level study, JHEP 1405 (2014) 060. [arXiv:1312.1566](#), doi:10.1007/JHEP05(2014)060.
- [52] D. Hesse, R. Sommer, A one-loop study of matching conditions for static-light flavor currents, JHEP 1302 (2013) 115. [arXiv:1211.0866](#), doi:10.1007/JHEP02(2013)115.
- [53] P. Korcyl, Fixing the parameters of Lattice HQET including $1/m_B$ terms, PoS Beauty2013 (2013) 071. [arXiv:1307.5080](#).
- [54] P. Korcyl, On one-loop corrections to matching conditions of Lattice HQET including $1/m_b$ terms, PoS Lattice2013 (2013) 380. [arXiv:1312.2350](#).
- [55] M. Della Morte, J. Heitger, H. Simma, R. Sommer, Non-perturbative Heavy Quark Effective Theory: An application to semileptonic B-decays, SFB TR9 - Computational Particle Physics, SFB/CPP-14-102.
- [56] M. Kurth, R. Sommer, Renormalization and $O(a)$ improvement of the static axial current, Nucl.Phys. B597 (2001) 488–518. [arXiv:hep-lat/0007002](#), doi:10.1016/S0550-3213(00)00750-1.
- [57] J. Balog, F. Niedermayer, P. Weisz, The Puzzle of apparent linear lattice artifacts in the 2d non-linear sigma-model and Symanzik's solution, Nucl.Phys. B824 (2010) 563–615. [arXiv:0905.1730](#), doi:10.1016/j.nuclphysb.2009.09.007.
- [58] J. Balog, F. Niedermayer, P. Weisz, Symanzik effective actions in the large N limit, JHEP 1308 (2013) 027. [arXiv:1304.6269](#), doi:10.1007/JHEP08(2013)027.
- [59] G. P. Lepage, Simulating heavy quarks, Nucl.Phys.Proc.Suppl. 26 (1992) 45–56. doi:10.1016/0920-5632(92)90228-K.
- [60] M. Lüscher, Computational Strategies in Lattice QCD., year = 331–399. [arXiv:1002.4232](#).
- [61] R. Sommer, Leptonic decays of B and D mesons, Nucl.Phys.Proc.Suppl. 42 (1995) 186–193. [arXiv:hep-lat/9411024](#), doi:10.1016/0920-5632(95)00201-J.
- [62] M. Della Morte, et al., Lattice HQET with exponentially improved statistical precision, Phys.Lett. B581 (2004) 93–98. [arXiv:hep-lat/0307021](#), doi:10.1016/j.physletb.2005.03.017.
- [63] M. Teper, An Improved Method for Lattice Glueball Calculations, Phys.Lett. B183 (1987) 345. doi:10.1016/0370-2693(87)90976-2.
- [64] Güsken, S. and Löw, U. and Mutter, K.H. and Sommer, R. and Patel, A. and others, Nonsinglet Axial Vector Couplings of the Baryon Octet in Lattice QCD, Phys.Lett. B227 (1989) 266. doi:10.1016/S0370-2693(89)80034-6.
- [65] C. Michael, I. Teasdale, Extracting Glueball Masses From Lattice QCD, Nucl.Phys. B215 (1983) 433. doi:10.1016/0550-3213(83)90674-0.
- [66] M. Luscher, U. Wolff, How to Calculate the Elastic Scattering Matrix in Two-dimensional Quantum Field Theories by Numerical Simulation, Nucl.Phys. B339 (1990) 222–252. doi:10.1016/0550-3213(90)90540-T.
- [67] B. Blossier, M. Della Morte, G. von Hippel, T. Mendes, R. Sommer, On the generalized eigenvalue method for energies and matrix elements in lattice field theory, JHEP 0904 (2009) 094. [arXiv:0902.1265](#), doi:10.1088/1126-6708/2009/04/094.
- [68] J. Bulava, M. Donnellan, R. Sommer, On the computation of hadron-to-hadron transition matrix elements in lattice QCD, JHEP 1201 (2012) 140. [arXiv:1108.3774](#), doi:10.1007/JHEP01(2012)140.
- [69] J. Heitger, A. Jüttner, R. Sommer, J. Wennekers, Non-perturbative tests of heavy quark effective theory, JHEP 0411 (2004) 048. [arXiv:hep-ph/0407227](#), doi:10.1088/1126-6708/2004/11/048.
- [70] N. G. Patrick Fritzsche, J. Heitger, Non-perturbative tests of continuum HQET through small-volume two-flavour QCD, in preparation.
- [71] J. Heitger, J. Wennekers, Effective heavy light meson energies in small volume quenched QCD, JHEP 0402 (2004) 064. [arXiv:hep-lat/0312016](#), doi:10.1088/1126-6708/2004/02/064.
- [72] M. Della Morte, P. Fritzsche, J. Heitger, Non-perturbative renormalization of the static axial current in two-flavour QCD, JHEP 0702 (2007) 079. [arXiv:hep-lat/0611036](#), doi:10.1088/1126-6708/2007/02/079.
- [73] M. Della Morte, et al., Simulating the Schrödinger functional with two pseudofermions, Comput.Phys.Commun. 156 (2003) 62–72. [arXiv:hep-lat/0307008](#), doi:10.1016/S0010-4655(03)00436-3.
- [74] R. Hoffmann, F. Knechtli, J. Rolf, R. Sommer, U. Wolff, Nonperturbative renormalization of the axial current with improved Wilson quarks, Nucl.Phys.Proc.Suppl. 129 (2004) 423–425. [arXiv:hep-lat/0309071](#), doi:10.1016/S0920-5632(03)02602-1.
- [75] M. Della Morte, R. Hoffmann, F. Knechtli, U. Wolff, Impact of large cutoff-effects on algorithms for improved Wilson fermions, Comput.Phys.Commun. 165 (2005) 49–58. [arXiv:hep-lat/0405017](#), doi:10.1016/j.cpc.2004.09.009.
- [76] M. Della Morte, R. Hoffmann, F. Knechtli, R. Sommer, U. Wolff, Non-perturbative renormalization of the axial current with dynamical Wilson fermions, JHEP 0507 (2005) 007. [arXiv:hep-lat/0505026](#), doi:10.1088/1126-6708/2005/07/007.
- [77] M. Della Morte, et al., Non-perturbative quark mass renormalization in two-flavor QCD, Nucl.Phys. B729 (2005) 117–134. [arXiv:hep-lat/0507035](#), doi:10.1016/j.nuclphysb.2005.09.028.
- [78] Coordinated lattice simulations, <https://twiki.cern.ch/twiki/bin/view/CLS/WebHome>.
- [79] P. Fritzsche, F. Knechtli, B. Leder, M. Marinkovic, S. Schaefer, et al., The strange quark mass and Lambda parameter of two flavor QCD, Nucl.Phys. B865 (2012) 397–429. [arXiv:1205.5380](#), doi:10.1016/j.nuclphysb.2012.07.026.
- [80] M. Hasenbusch, Speeding up the hybrid Monte Carlo algorithm for dynamical fermions, Phys.Lett. B519 (2001) 177–182. [arXiv:hep-lat/0107019](#), doi:10.1016/S0370-2693(01)01102-9.
- [81] M. Hasenbusch, K. Jansen, Speeding up lattice QCD simulations with clover improved Wilson fermions, Nucl.Phys. B659 (2003) 299–320. [arXiv:hep-lat/0211042](#), doi:10.1016/S0550-3213(03)00227-X.
- [82] Lüscher, Martin, Deflation acceleration of lattice QCD simulations, JHEP 0712 (2007) 011. [arXiv:0710.5417](#), doi:10.1088/1126-6708/2007/12/011.
- [83] Lüscher, Martin, Local coherence and deflation of the low quark modes in lattice QCD, JHEP 0707 (2007) 081. [arXiv:0706.2298](#), doi:10.1088/1126-6708/2007/07/081.
- [84] M. Marinkovic, S. Schaefer, Comparison of the mass precon-

- ditioned HMC and the DD-HMC algorithm for two-flavour QCD, PoS LATTICE2010 (2010) 031. [arXiv:1011.0911](#).
- [85] A. Frommer, K. Kahl, S. Krieg, B. Leder, M. Rottmann, Adaptive Aggregation Based Domain Decomposition Multigrid for the Lattice Wilson Dirac Operator, SIAM J.Sci.Comput. 36 (2014) A1581–A1608. [arXiv:1303.1377](#), doi:10.1137/130919507.
- [86] I. Omelyan, I. Mryglod, R. Folk, Symplectic analytically integrable decomposition algorithms: classification, derivation, and application to molecular dynamics, quantum and celestial mechanics simulations, Computer Physics Communications 151 (3) (2003) 272 – 314. doi:[http://dx.doi.org/10.1016/S0010-4655\(02\)00754-3](#).
- [87] S. Duane, A. Kennedy, B. Pendleton, D. Roweth, Hybrid Monte Carlo, Phys.Lett. B195 (1987) 216–222. doi:10.1016/0370-2693(87)91197-X.
- [88] S. A. Gottlieb, W. Liu, D. Toussaint, R. L. Renken, R. L. Sugar, Hybrid Molecular Dynamics Algorithms for the Numerical Simulation of Quantum Chromodynamics, Phys. Rev. D35 (1987) 2531. doi:10.1103/PhysRevD.35.2531.
- [89] Lüscher, Martin, Computational Strategies in Lattice QCD (2010) 331–399 [arXiv:1002.4232](#).
- [90] S. Schaefer, Status and challenges of simulations with dynamical fermions, PoS LATTICE2012 (2012) 001. [arXiv:1211.5069](#).
- [91] R. Sommer, U. Wolff, Non-perturbative computation of the strong coupling constant on the lattice, SFB TR9 - Computational Particle Physics, report SFB/CPP-14-100.
- [92] F. Bernardoni, J. Bulava, M. Donnellan, R. Sommer, Precision lattice QCD computation of the $B^*B\pi$ coupling, Physics Letters B 740 (0) (2015) 278 – 284. [arXiv:1404.6951](#), doi:[http://dx.doi.org/10.1016/j.physletb.2014.11.051](#).
- [93] H. Ohki, H. Matsufuru, T. Onogi, Determination of $B^*B\pi$ coupling in unquenched QCD, Phys.Rev. D77 (2008) 094509. [arXiv:0802.1563](#), doi:10.1103/PhysRevD.77.094509.
- [94] D. Becirevic, B. Blossier, E. Chang, B. Haas, $g(B^*B\pi)$ -coupling in the static heavy quark limit, Phys. Lett. B679 (2009) 231–236. [arXiv:0905.3355](#), doi:10.1016/j.physletb.2009.07.031.
- [95] W. Detmold, C. D. Lin, S. Meinel, Calculation of the heavy-hadron axial couplings g_1 , g_2 , and g_3 using lattice QCD, Phys.Rev. D85 (2012) 114508. [arXiv:1203.3378](#), doi:10.1103/PhysRevD.85.114508.
- [96] G. Burdman, J. F. Donoghue, Union of chiral and heavy quark symmetries, Phys.Lett. B280 (1992) 287–291. doi:10.1016/0370-2693(92)90068-F.
- [97] M. B. Wise, Chiral perturbation theory for hadrons containing a heavy quark, Phys.Rev. D45 (1992) 2188–2191. doi:10.1103/PhysRevD.45.R2188.
- [98] T.-M. Yan, H.-Y. Cheng, C.-Y. Cheung, G.-L. Lin, Y. Lin, et al., Heavy quark symmetry and chiral dynamics, Phys.Rev. D46 (1992) 1148–1164. doi:10.1103/PhysRevD.46.1148, 10.1103/PhysRevD.55.5851.
- [99] B. Blossier, M. della Morte, N. Garron, R. Sommer, HQET at order $1/m$: I. Non-perturbative parameters in the quenched approximation, JHEP 1006 (2010) 002. [arXiv:1001.4783](#), doi:10.1007/JHEP06(2010)002.
- [100] M. Della Morte, et al., Computation of the strong coupling in QCD with two dynamical flavors, Nucl.Phys. B713 (2005) 378–406. [arXiv:hep-lat/0411025](#), doi:10.1016/j.nuclphysb.2005.02.013.
- [101] M. Della Morte, R. Sommer, S. Takeda, On cutoff effects in lattice QCD from short to long distances, Phys.Lett. B672 (2009) 407–412. [arXiv:0807.1120](#), doi:10.1016/j.physletb.2009.01.059.
- [102] P. Fritzsch, J. Heitger, N. Tantalo, Non-perturbative improvement of quark mass renormalization in two-flavour lattice QCD, JHEP 1008 (2010) 074. [arXiv:1004.3978](#), doi:10.1007/JHEP08(2010)074.
- [103] S. M. Ryan, Heavy quark physics from lattice QCD, Nucl.Phys.Proc.Suppl. 106 (2002) 86–97. [arXiv:hep-lat/0111010](#), doi:10.1016/S0920-5632(01)01647-4.
- [104] M. Della Morte, N. Garron, M. Papinutto, R. Sommer, Heavy quark effective theory computation of the mass of the bottom quark, JHEP 0701 (2007) 007. [arXiv:hep-ph/0609294](#), doi:10.1088/1126-6708/2007/01/007.
- [105] F. Bernardoni, B. Blossier, J. Bulava, M. Della Morte, P. Fritzsch, et al., The b-quark mass from non-perturbative $N_f = 2$ Heavy Quark Effective Theory at $O(1/m_b)$, Phys.Lett. B730 (2014) 171–177. [arXiv:1311.5498](#), doi:10.1016/j.physletb.2014.01.046.
- [106] G. Martinelli, C. T. Sachrajda, Computation of the b quark mass with perturbative matching at the next-to-next-to-leading order, Nucl.Phys. B559 (1999) 429–452. [arXiv:hep-lat/9812001](#), doi:10.1016/S0550-3213(99)00423-X.
- [107] H. Trotter, N. Shakespeare, G. Lepage, P. Mackenzie, Perturbative expansions from Monte Carlo simulations at weak coupling: Wilson loops and the static quark selfenergy, Phys.Rev. D65 (2002) 094502. [arXiv:hep-lat/0111028](#), doi:10.1103/PhysRevD.65.094502.
- [108] F. Di Renzo, L. Scorzato, The Residual mass in lattice heavy quark effective theory to α_s^3 order, JHEP 0102 (2001) 020. [arXiv:hep-lat/0012011](#), doi:10.1088/1126-6708/2001/02/020.
- [109] K. Olive, et al., Review of Particle Physics, Chin.Phys. C38 (2014) 090001. doi:10.1088/1674-1137/38/9/090001.
- [110] B. Blossier, et al., HQET at order $1/m$: III. Decay constants in the quenched approximation, JHEP 1012 (2010) 039. [arXiv:1006.5816](#), doi:10.1007/JHEP12(2010)039.
- [111] R. Sommer, A New way to set the energy scale in lattice gauge theories and its applications to the static force and α_s in SU(2) Yang-Mills theory, Nucl.Phys. B411 (1994) 839–854. [arXiv:hep-lat/9310022](#), doi:10.1016/0550-3213(94)90473-1.
- [112] R. Sommer, Beauty physics in lattice gauge theory, Phys. Rept. 275 (1996) 1–47. [arXiv:hep-lat/9401037](#).
- [113] F. Bernardoni, et al., Decay constants of B-mesons from non-perturbative HQET with two light dynamical quarks, Phys.Lett. B735 (2014) 349–356. [arXiv:1404.3590](#), doi:10.1016/j.physletb.2014.06.051.
- [114] Y. Aoki, T. Ishikawa, T. Izubuchi, C. Lehner, A. Soni, Neutral B meson mixings and B meson decay constants with static heavy and domain-wall light quarks [arXiv:1406.6192](#).
- [115] S. Aoki, Y. Aoki, C. Bernard, T. Blum, G. Colangelo, et al., Review of lattice results concerning low-energy particle physics, Eur.Phys.J. C74 (9) (2014) 2890. [arXiv:1310.8555](#), doi:10.1140/epjc/s10052-014-2890-7.
- [116] K. Bowler, et al., Decay constants of B and D mesons from nonperturbatively improved lattice QCD, Nucl.Phys. B619 (2001) 507–537. [arXiv:hep-lat/0007020](#), doi:10.1016/S0550-3213(01)00511-9.
- [117] R. Sommer, Scale setting in lattice QCD, PoS LATTICE2013 (2014) 015. [arXiv:1401.3270](#).
- [118] C. Albertus, Y. Aoki, P. Boyle, N. Christ, T. Dumitrescu, et al., Neutral B-meson mixing from unquenched lattice QCD with domain-wall light quarks and static b-quarks, Phys.Rev. D82 (2010) 014505. [arXiv:1001.2023](#), doi:10.1103/PhysRevD.82.014505.
- [119] T. Burch, C. Hagen, C. B. Lang, M. Limmer, A. Schafer, Excitations of single-beauty hadrons, Phys. Rev. D79 (2009)

014504. [arXiv:0809.1103](#).
- [120] M. Bruno, J. Finkenrath, F. Knechtli, B. Leder, R. Sommer, On the effects of heavy sea quarks at low energies. [arXiv:1410.8374](#).
 - [121] B. Blossier, et al., HQET at order $1/m$: II. Spectroscopy in the quenched approximation, JHEP 1005 (2010) 074. [arXiv:1004.2661](#), doi:10.1007/JHEP05(2010)074.
 - [122] M. Bruno, D. Djukanovic, G. P. Engel, A. Francis, G. Herdoiza, et al., Simulation of QCD with $N_f = 2+1$ flavors of non-perturbatively improved Wilson fermions [arXiv:1411.3982](#).
 - [123] F. Bahr, et al., $|V_{ub}|$ determination in lattice QCD, PoS ICHEP2012 (2013) 424. [arXiv:1211.6327](#).
 - [124] F. Bahr, F. Bernardoni, A. Ramos, H. Simma, R. Sommer, et al., $B \rightarrow \pi$ form factor with 2 flavours of $O(a)$ improved Wilson quarks, PoS LATTICE2012 (2012) 110. [arXiv:1210.3478](#).
 - [125] F. Bahr, F. Bernardoni, J. Bulava, A. Joseph, A. Ramos, et al., Form factors for $B_s \rightarrow K\ell\nu$ decays in Lattice QCD [arXiv:1411.3916](#).